COST OPTIMIZATION OF A SOLAR-POWERED ELECTRODIALYSIS DESALINATION SYSTEM

by

Sterling M. Watson

S.B. in Mechanical Engineering
Massachusetts Institute of Technology, 2015

Submitted to the
Department of Mechanical Engineering
in partial fulfillment of the requirements for the degree of
Master of Science in Mechanical Engineering

at the

MASSACHUSETTS INSTITUTE OF TECHNOLOGY

June 2017

Author: ..... Signature redacted
Department of Mechanical Engineering
May 12, 2017

Certified by: ..... Signature redacted
Tonio Buonassisi
Associate Professor of Mechanical Engineering
Thesis Co-Supervisor

Signature redacted
....
Ian Marius Peters
Research Scientist in Mechanical Engineering
Thesis Co-Supervisor

..... Signature redacted .....
Amos Winter
Assistant Professor of Mechanical Engineering
Thesis Co-Supervisor

Accepted by: ..... Signature redacted .....
Rohan Abeyaratne
Professor of Mechanical Engineering
Chairman, Committee on Graduate Students

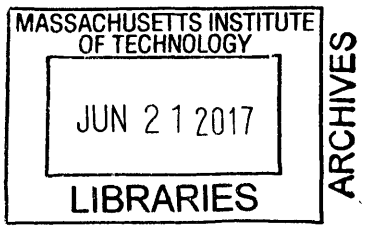

Cost Optimization of a Solar-Powered Electrodialysis Desalination System

by

Sterling M. Watson

Submitted the Department of Mechanical Engineering
on May 12, 2017 in Partial Fulfillment of the
Requirements for the Degree of Master of Science in
Mechanical Engineering

ABSTRACT

With their autonomous operation and low environmental impact, solar photovoltaics (PV) are an attractive power source for off-grid systems. One application of PV is for powering village-scale desalination systems, which are needed in regions with a saline drinking water supply and an unreliable electric grid. However, the intermittent and non-dispatchable nature of solar energy is not well-suited to conventional loads that are designed to operate off of a steady electrical grid, so it is important to design and optimize PV-powered systems such that they are persistent, reliable, predictable, and low-cost.

In this thesis, I present a solar photovoltaic-powered electrodialysis reversal (PV-EDR) model, and use it to design a steady voltage and pumping EDR system composed of current off-the-shelf parts for Chelluru, a village near Hyderabad, India. I investigate flexible operation and load sizing as design approaches for low-cost PV-powered systems, and apply these concepts to a

theoretical reference system and the PV-EDR system. I also present the results of a 7-day field test of the PV-EDR system in Chelluru.

Through a sensitivity analysis performed with the PV-EDR model, I found that easing the output reliability constraint for the PV-EDR system from 100% to 98% reduced the system capital cost by 5.7%, indicating that usage of alternative water supplies during brief and infrequent periods of low sunshine could be a cost-effective way of supplementing PV-EDR if constant water production is required year-round. I found that the capital cost of the PV-EDR system was highly sensitive to the cost of the PV-EDR membranes, and foreseeable membrane cost reductions of 87% could reduce the cost of the total system by 50%. This observation was reaffirmed through an analysis of the effect of flexible operation and load sizing for PV-powered systems, which revealed that if the electrical load can be designed to operate primarily during the sunny hours of the day (as would be the case for a larger EDR unit enabled by inexpensive membranes), the PV and batteries could be downsized compared to a system that operates through the night.

The PV-EDR model presented in this thesis was found to predict the operation of the installed system within 13% for the 7-day village test. This model can be adapted to other PV-powered systems to aid in design and cost optimization, and its accuracy will be further improved through additional testing and improved PV and battery device models. The flexible operation and load sizing design approaches detailed in this thesis will be useful for informing the design of any PV-powered system with accumulable output.

Thesis Supervisors:
Tonio Buonassisi, Associate Professor of Mechanical Engineering
Amos Winter, Assistant Professor of Mechanical Engineering
Marius Peters, Research Scientist in Mechanical Engineering

ACKNOWLEDGEMENTS

I would like to thank my advisors in the PVLab and the GEAR Lab for their guidance and support throughout this project. I have benefitted tremendously from the wisdom and direction that Professor Tonio Buonassisi has shared with me, and I am tremendously inspired by his vision and dedication pushing for solar photovoltaics technologies and adoption forward. I am also so grateful for the guidance and assistance that Marius Peters has given me throughout all stages of this project, from project formulation, to technical details, to the writing of this thesis. My advisors in the PVLab have been indispensable in pointing my research in a fruitful direction and helping me over countless hurdles throughout the pursuit of my master's degree. I am truly grateful for the PVLab community and the professional relationships and friendships that I have formed as a part of this group.

I would also like to thank Professor Amos Winter for the wonderful opportunity to design, install, and field-test a PV-EDR system as a member of the GEAR Lab. I have learned so much from him as a teacher and a mentor, and talking with him has never failed to renew my excitement to be an engineer. Natasha Wright has been an incredible inspiration to me, and it has been an honor to work with her at MIT and during our field work in India. I truly cannot thank my research partner, David Bian, enough for the dedication that he has put into this project, and his commitment to being an exceptional team member. It is due to his unfailing hard work that our PV-EDR system is operational in the field today. As a whole, GEAR Lab is a remarkable, supportive community making incredible engineering impact in the developing world, and I have learned so much from them.

I am very grateful to have been a co-advised student in the PV and GEAR Labs at MIT. It has allowed me to combine my passions for renewable energy systems and global impact, and having access to the expertise of both groups has put me in the best position to develop my understanding and knowledge of PV-powered systems. This work has benefitted tremendously from the excellent team at Tata Projects, who helped us in every detail of field testing and who share a passion for making PV-powered desalination the standard in India's villages. I would also

like to thank our partners at the Singapore-MIT Alliance for Research and Technology (SMART), in particular Nasim Sahraei.

Finally, I would like to thank the sponsors of this research and my graduate studies: Tata Projects Ltd., USAID, the MIT Energy Initiative (MITEI), the MIT Tata Center for Technology and Design, and the MIT Presidential Fellowship.

ACKNOWLEDGEMENT OF JOINT WORK

This project was done jointly with David Bian as part of a collaboration between the PVLab and GEAR Lab. Our theses were prepared in parallel and share much of the same content, but have been crafted to highlight each of our individual contributions.

CONTENTS

LIST OF FIGURES

LIST OF TABLES

CHAPTER 1

INTRODUCTION

This thesis investigates design approaches for building persistent, reliable, predictable, and affordable PV-powered systems, and applies these concepts in the design of a cost-optimized, off-grid, village-scale, solar photovoltaic-powered electrodialysis reversal (PV-EDR) desalination system. This PV-EDR system was built, installed, and field-tested in Chelluru, a village near Hyderabad, India. In this work, I investigate the effects that operation flexibility and load sizing,

two methods of improving the suitability of an electrical load to PV power, have on the total cost of PV-powered systems, and I use these learnings to recommend future work in PV-EDR system design. The results and contributions of this work are the following:

- Demonstration of a PV-EDR model
- Presentation of a cost-optimized PV-EDR system design composed of currently-available off-the-shelf components
- Investigation of the cost reductions enabled by flexible operation and load sizing for generalized PV-powered systems
- Installation and results from a PV-EDR field test in Chelluru, India.

1.1 Motivation for PV-Powered System Optimization

Solar photovoltaics (PV) represent an autonomous and environmentally benign power source for off-grid systems. According to the World Bank, 27% of the global rural population lacked electricity access in 2014 [1]. Solar is the most abundant renewable energy source, and can play a key role in mitigating anthropogenic carbon emissions and climate change while also serving as a low-maintenance energy source for regions without a reliable grid connection. While PV modules have historically been cost-prohibitive in many applications, particularly in the developing world, PV module prices have declined by 10x during the last decade, enabling their use in these new markets.

However, adapting existing systems to PV power in a cost-effective and reliable way is not always straightforward. While conventional energy sources and grid electricity are dispatchable and non-intermittent, PV is naturally intermittent and non-dispatchable [2]. An electrical load designed to operate on a continuous conventional energy source requires adaptation to operate with a variable PV power source. A storage medium can buffer the variability of the PV power source, rendering solar power predictable and persistent [3] [4].

A key challenge in the field of PV-powered systems is to create systems that are simultaneously low-cost and sufficiently non-intermittent. Inadequate system design yields either higher cost (over-design) or lower reliability (under-design) [5]. Low cost and high reliability are desired features for PV-powered systems, particularly in the developing world. On the other hand,

co-design (as opposed to independent, disaggregated design) of the PV subsystem, storage media, and electrical load represents an opportunity for deep cost reductions and technological innovation. Furthermore, an opportunity exists to template key learnings in a system-design framework, to enable rapid development of a wide range of future optimized PV-powered systems. Cost reductions through system optimization are essential to accelerating PV-powered system adoption in low-income, off-grid environments [6] [7].

1.2 Motivation for Off-Grid, Village-Scale Electrodialysis Desalination

There is a global deficiency of safe drinking water sources, despite the existence of technologies that can purify or desalinate a local water supply. In 2015, the WHO / UNICEF Joint Monitoring Programme (JMP) for Water Supply and Sanitation reported that nine percent of the global population, or 663 million people—close to the number of people living in the European Union—do not use an improved drinking water source [8]. In India, dissolved salts are a primary contaminant of the groundwater supply, and brackish groundwater (defined as water with a total dissolved solids content (TDS) between 500 and 30,000 mg/L) underlies approximately 60% of the land area (Figure 1) [9]. The Bureau of Indian Standards for Drinking Water has set the acceptable upper limit for TDS to 500 mg/L for improved palatability and minimal risk of gastrointestinal irritation [10]. Desalination is required to make brackish groundwater an acceptable drinking water source.

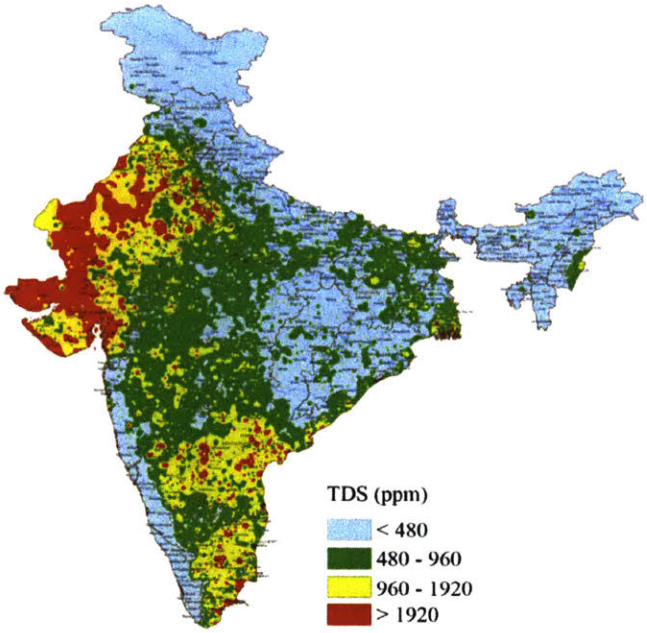

Figure 1. Map of Groundwater Salinity Levels Throughout India

Regions colored red, yellow, or green have brackish groundwater above the taste threshold. [9]

In 2015, 96.7% of villages in India had some form of grid electricity [11]. However, the grid electricity in most villages is not reliable, nor do many households benefit from it. In 2011, only 55.3% of rural households used electricity for lighting [12], implying that not all households in electrified villages have reliable access to basic electricity. Even those that do have access to electricity experience intermittent power outages, and may only have access for a few hours a day. Because of the limitations of the current electrical grid, grid-powered desalination is not viable for much of India's rural population.

Grid-reliant desalination systems must be designed to meet the daily water needs of a village within the limited number of hours for which grid access is available [13]. For example, if a village requires 10,000 liters of water and has 5 hours of grid electricity per day, then the production rate of the desalination system must be 2,000 liters per hour (LPH). If the village has only 1 hour of reliable electricity, then the desalination system must have a production rate of 10,000 LPH. Because the capital cost of a desalination system roughly scales with the water production rate, there is an economic capital cost incentive to run for longer periods of time.

Despite the challenges of implementing desalination in rural settings, expanding to this subsection of the population is critical for meeting the drinking water needs of villages without reliable grid access. Based on maps compiled by the Central Groundwater Board of India, it has been concluded that village-scale desalination, in addition to other purification methods, could at least double the land area for which groundwater can acceptably be used as drinking water in India [13].

Because of the constraints of an unreliable grid, PV-powered desalination systems have become more attractive. This is particularly the case in India, where solar energy is readily available and water consumption is correlated with solar irradiance [13]. Solar energy is locally and indefinitely available, eliminating the need for consumable fuels such as diesel. PV panels also operate silently and without pollution to the environment and require minimal maintenance. However, the addition of a PV power system to a desalination unit significantly increases the capital cost of the total system. When comparing similar capacity systems designed for on-grid and off-grid operation, the cost of the off-grid, PV-powered reverse osmosis (PV-RO) system is more than double that of the on-grid system. According to an Indian OEM infrastructure company that has installed over 2,000 RO systems in the field, an on-grid 500 LPH RO system costs approximately $4,500, while an equivalent unit equipped with a PV power system costs $11,250 [14]. To make off-grid desalination systems economically feasible, it is necessary to reduce the cost of the PV power system.

One way to reduce the cost of the PV power system is to reduce the power requirements of the desalination unit. Electrodialysis (ED) is a desalination technology that separates salts from water by inducing movement of ions across semi-permeable ion-exchange membranes through the application of an electric potential. Electrodialysis reversal (EDR) is a variant of ED that periodically switches the polarity of the applied voltage to reduce salt buildup and extend membrane life. ED is expected to have a lower specific energy of desalination than RO for brackish water salinities below 5,000 mg/L. In fact, ED may require less than 50% of the energy used by RO to desalinate water below 2,000 mg/L, which represents the majority of India's brackish groundwater [13]. These factors suggest that ED could provide a low-cost, off-grid brackish water desalination solution [15].

1.3 Prior Art

1.3.1 Previous Work on PV System Optimization

Previous work in the field of PV system optimization has focused on optimal power system sizing through simulation of electrical loads, power management, and PV power generation. Cost-optimized PV power systems for various applications have been studied and tested [16] [17] [18] [19] [20]. The techno-economic optimization of a PV power system for water pumping in Antalya, Turkey was studied by Olcan et al [16]. The optimization was dual-objective and focused on minimizing the deficiency of power supply probability (DPSP) and the life-cycle costs. This study used a similar method of operating flexibly and using a water storage tank as buffer. However, the benefit of the flexible schedule was not characterized, and the pumping load was fixed. The optimal sizing of a different PV water pumping system with water storage for remote villages in Algeria was also investigated in Bakelli et al [17].

In Bilton et al [21], an optimization was used to determine the most economical off-grid reverse osmosis (RO) desalination system sizing considering PV, wind, and diesel energy sources, as well as the sizing of the RO system and water storage. Flexible operation and load sizing are intrinsic to this analysis as well as the work of others seeking to optimize off-grid RO powered by multiple energy sources, but the benefits of flexible scheduling and load sizing for PV have not been characterized [21] [22] [23] [24]. A PV-wind-fuel cell RO unit was optimized in Smaoui et al, but the benefits of load scheduling were also not investigated [22].

Habib et al [25] optimized the sizing of the PV power system as well as the sizing and scheduling of electrical loads in a microgrid. The purpose of that work was to maximize solar energy utilization by scheduling loads accordingly. That approach, while in some respects similar to the work presented here, focused on the scheduling of multiple loads in the microgrid setting, rather than the optimization of a single PV-powered load. Load scheduling for a PV-powered microgrid was also investigated by Jaramillo et al [26]. The effect of temporal resolution on the sizing of an optimized PV-battery system has also been investigated previously [27].

1.3.2 Previous Work on PV-Powered Desalination System Design

The use of PV power for ED and EDR systems has been studied in the past. Laboratory scale work has been completed to model and test a PV-ED system (Ortiz 2006). A number of field

pilots have also been conducted. In 1987, Adiga et. al. [28] completed a pilot PV-ED project with a production rate of 0.12 m^3/hr in the Thar Desert. However, the water was only desalinated from 5,000 mg/L to 1,000 mg/L, well above the 500 mg/L drinking water requirement. Because of the low charging and storage efficiency of batteries at the time, and associated high cost of a suitably sized PV system, batteries were omitted and the PV-ED system was designed to exclusively operate during daylight hours (8:30AM – 4:30PM). In the same year, Kuroda et al. [29] designed and constructed a batch mode PV-ED seawater desalination system in Nagasaki where they produced 2-5 m^3 of drinking water daily and aimed to optimize the system by matching its power consumption to the power generation of the PV panels. A few years later, Soma et al. [30] constructed a similar PV-ED system for brackish water desalination, and monitored the seasonal variation of water production. Both systems were motivated by the desire to reduce the cost of PV-ED desalination, but the tests were conducted about thirty years ago, produced water of a higher salinity than our targets for an Indian village, and listed no concrete cost values. Additionally, advancements in PV and battery technology have enabled different PV-ED configurations and at lower costs than what was previously achievable.

Cost optimization of PV-powered reverse osmosis (RO) desalination systems is a related area of research. Bilton et al. [31] investigated the impacts of location-specific environmental and demand parameters on the optimal design of modular PV-RO desalination systems using genetic algorithms. Bilton et al. [32] have also worked extensively on examining energy generation methods considering not only PV, but also wind turbines and diesel generators, and optimizing them together with RO systems to determine a high-reliability system configuration with the lowest lifecycle cost. The work presented in this thesis has similar goals in optimizing for minimal system cost while achieving high reliability of off-grid desalination systems in underserved communities. However, the performance and costs of components such as solar panels and batteries are generalized, rather than picking specific components from an inventory. Furthermore, this optimization analysis is focused on a single location, and the pilot system was designed and built to evaluate its performance in the field. Nonetheless, the approach presented here can be generalized for other applications.

While much work has been done to understand the process of ED, it has mostly been limited to the laboratory in recent years. The field-tested Thar Desert and Nagasaki systems are

similar to the work presented here in that they were both motivated by reducing the cost of PV-ED desalination, but the tests were done about thirty years ago, produced a smaller volume of water at a higher salinity than our targets for an Indian village, and listed no concrete cost values. Additionally, advancements in PV and battery technology have enabled different PV-ED configurations at lower cost than what was achievable previously.

1.3.3 Objectives and Scope

This thesis presents the benefits of flexible operation and optimal load sizing of a generalized off-grid, PV-powered process producing an accumulable output, as well as the application of these ideas to a field-tested PV-EDR desalination system. Here, the term "flexible operation" refers to process insensitivity to operating schedule, while "optimal load sizing" is the ability to design the load to operate at different power levels that complete the desired task over a corresponding duration.

This thesis presents the parametric theory to design a cost-minimized constant voltage and pumping power PV-EDR system that can be built from off-the-shelf parts. We used GE Water's electrodialysis stack Model Number AQ3-1-2-50/35, which was previously studied, modeled and tested by Wright et al. [13], and was readily available for this work. We chose to operate with constant voltage and constant pumping power to match the way in which ED is conventionally run, and we used off-the-shelf parts, current cost estimates, and current performance estimates to establish a baseline for what is currently possible to build. We can use the findings from a PV-EDR system with these characteristics to understand the cost sensitivities and decide where future research should be focused to enable further cost reductions. The theory, observations, and results from this work will aid engineers in designing cost-effective PV-powered systems for other size scales and contexts.

For the PV-EDR pilot, we designed, installed, and tested a low-cost PV-EDR system composed of off-the-shelf components to meet the drinking water needs of Chelluru, a village near Hyderabad, India. Chelluru was selected for the PV-EDR pilot test because it has a characteristic village size between 2,000 and 5,000 people, a groundwater salinity of 1,600 mg/L (within the typical Indian range of 1,000-2,000 mg/L and well-suited for ED compared to RO), and has been operating a grid-connected RO system which can be compared head-to-head with our off-grid EDR system in long-term tests. The PV-EDR system was designed to produce 10 m^3 per day of

300 mg/L drinking water. This production rate was based on the median Indian village water consumption (10 m^3 per day), and the TDS level of 300 mg/L was selected for increased palatability, well below the Bureau of Indian Standards for Drinking Water recommendation of 500 mg/L.

1.4 Approach

In this thesis, I investigate the sensitivities and tradeoffs of PV-powered systems and apply the learnings to design, install, and test an off-grid, village-scale, cost-optimized PV-EDR desalination system for Chelluru, India. I show that allowing for flexible system operation—as opposed to continuous non-intermittent operation—can further reduce the overall cost of PV-powered systems, by partially accommodating the natural time-variance of PV power [33]. System cost can be reduced by decreasing the required storage capacity and PV array size. I also explore the cost reductions enabled by flexible load sizing, or the design of the electrical load to operate over an optimal time period, to accommodate the diurnal and intermittent nature of solar energy.

To design the PV power system, I use local solar irradiance and temperature data from 2014 [34], a PV efficiency model, and an energy flow calculation. I also assess the tradeoffs between quantity of PV, batteries, and water storage to provide 100% output reliability for the 2014 reference year. I apply the concepts of flexible operation and load sizing to a theoretical reference PV-powered system to analyze the cost reductions enabled by these techniques.

I couple the PV power system model to an electrodialysis reversal (EDR) desalination model which considers various configurations of EDR components and input water salinities and produces the desalination power profiles and water output. The comprehensive PV-EDR model is coupled to a particle swarm optimization (PSO) which I use to determine the lowest-cost PV-EDR design that can meet the village drinking water needs. I also investigate the sensitivities of the PV-EDR system cost to changes in component cost and output reliability.

Through a cost-driven analysis, I demonstrate the cost-reduction benefits of (1) accommodating reasonable flexibility in the time-variance of system output, and (2) co-designing the electrical load with the PV power system such that the electrical load is well-suited to the PV power source. I demonstrate that flexible operation enables a power system cost reduction of 39%

for a reference system operating 8 hours per day at 1 kilowatt, while designing the electrical load to operate for an optimal period of time enables an additional power system cost reduction of 5%. For the desalination system, a power system cost reduction of 57.5% is made possible when sizing the desalination load to better overlap with the PV power source compared to the cost-optimized system described in Chapter 3.

Finally, I describe the design and field testing of the PV-EDR system in Chelluru, and use the experimental results to validate and tune my model. I use these learnings to recommend future work in PV-powered system design generally, as well as PV-EDR design specifically.

1.5 Structure of Thesis

In Chapter Two, I discuss the theory behind PV-powered systems and the energy analysis associated with the PV power output, battery energy storage, and power used by the electrical load. I also introduce the theoretical reference system and the product storage medium, and detail the physical process of EDR desalination in the context of its impact on system design. In Chapter Three, I describe the EDR model and its constitutive parts, as well as the PV-EDR system optimization performed to design the Chelluru village pilot, and the sensitivities of the optimized design to output reliability and individual component costs. In Chapter Four, I discuss the advantages of operation flexibility and load sizing for the theoretical reference system and the PV-EDR system. In Chapter Five, I present the results of the field-tested PV-EDR system and their implications for the model and design approach presented in this thesis. Finally, a discussion of the learnings and recommendations for future work are detailed in Chapter Six.

CHAPTER 2

THEORY

A solar-powered system with accumulable output is any system in which an electrical load is powered by PV to produce an output that can be stored. The relevant example discussed in this work is desalination, which produces storable drinking water as accumulable output. Other processes for which the same approach could be used include pumped water, drip irrigation, or any other process that uses energy to transform an input into a product and is indifferent to the time of day in which it is operated. In this chapter, I introduce a theoretical reference system and a PV-EDR system, and present the theory required to develop my power system and PV-EDR models.

2.1 Solar-Powered Systems with Accumulable Output

2.1.1 The Theoretical Reference System

As a reference system, we consider a design consisting of a 1 kW electrical load, producing an arbitrary accumulable output while operating 8 hours per day from 8am to 4pm; a PV array; and a battery bank (Figure 2). The PV array supplies power to the electrical load and the battery bank depending on the demands of each and the solar power available, and the electrical load produces an accumulable output that can be stored.

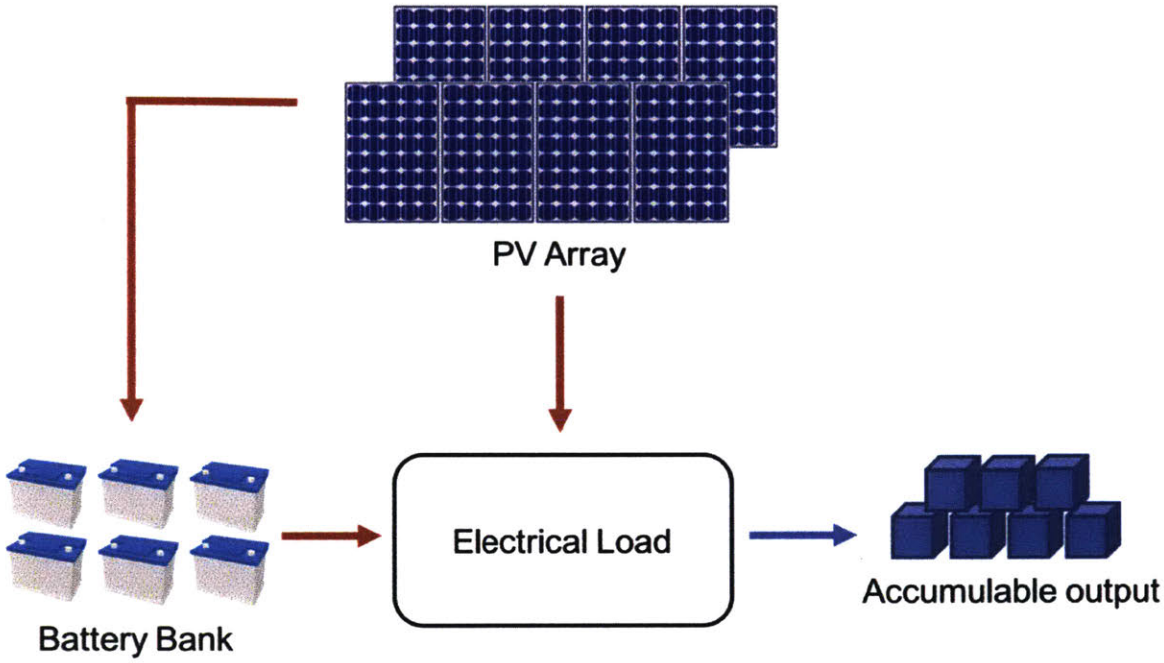

Figure 2. The Theoretical Reference System

The theoretical reference system consisting of a 1 kW electrical load producing an accumulable output from 8 am to 4 pm daily; a PV array; and a battery bank. The PV array powers the load directly and charges the battery if possible when the sun is shining. During times of low sunlight, the batteries power the load.

2.1.2 Energy Analysis

The power production of the PV array and the power usage of the electrical load were used to determine the sizing of the battery bank through an energy analysis. In this section, I describe

how the PV power output was calculated, and given an electrical load power profile, I explain how the energy storage requirement is calculated.

Solar irradiance and temperature data for the region of Chelluru, India, in the year 2014 was used as a reference year's weather data throughout this thesis. This is semi-empirical satellite-based data from NSRDB [34]. The efficiency of the solar panels at each time interval, η_{PV}, was calculated using Equation (*1*),

$$\eta_{PV}(t) = \eta_{PV,nom} \cdot \left(1 + \alpha_p \cdot (T_{amb}(t) + k \cdot GHI(t) - T_{std})\right), \quad (1)$$

where $\eta_{PV,nom}$ is the nominal efficiency of the panels (15%), α_p is the temperature coefficient ($\alpha_p = -0.42\%$ [35]), $T_{amb}(t)$ is the ambient temperature, k is the Ross coefficient, which relates irradiance to module temperature (k = 0.025 °C m^2/W [36]), $GHI(t)$ is the global horizontal irradiance, and T_{std} is the standard testing temperature (25 Celsius). The power produced by one square meter of PV, $P_{PV,1m}$, was calculated by multiplying the instantaneous PV efficiency, η_{PV}, by the instantaneous global horizontal irradiance $GHI(t)$. The PV array power output, P_{PV}, is simply the product of $P_{PV,1m}$ and the area of the PV array, A_{PV}.

The energy stored in the battery bank during charging was calculated according to Equation (*2*), and the energy stored during discharging was calculated according to Equation (*3*),

$$E_{stored}(t) = E_{stored}(t-1) + t_{int} \cdot \left(P_{PV}(t) - \frac{P_{load}(t)}{\eta_{conv}}\right) \cdot \eta_{batt}, \text{ and} \quad (2)$$

$$E_{stored}(t) = E_{stored}(t-1) - t_{int} \cdot \left(\frac{P_{load}(t)}{\eta_{conv}} - P_{PV}(t)\right), \quad (3)$$

where E_{stored} is the energy stored in the batteries, t_{int} is the interval length in seconds (300 seconds in this analysis), P_{load} is the power being consumed by the load, η_{conv} is the efficiency of the power converter, and η_{batt} is the battery charge/discharge efficiency (85%) [38]. Temperature effects were not considered in the battery operation, which is suitable for this PV-EDR system because the battery bank is stored indoors.

2.2 Relationship Between PV and Batteries

To understand the relationship between PV and batteries, I utilized the theoretical reference system of Figure 2, with a constant 1 kW power consumption from 8am to 4pm. I used solar irradiance and temperature data from Chelluru for 2014 as an input to the energy calculations. The costs of PV panels and batteries used in this analysis are \$98 per m^2 and \$150 per kWh, respectively, which are characteristic costs in India for multicrystalline silicon PV panels and lead acid batteries [39]. As a first-order constraint, the amount of PV panels must be enough to produce the total amount of energy required to desalinate water over the yearly cycle. This minimum PV area, $A_{PV,min}$, can be found by taking the total energy required to desalinate a year's worth of water and dividing by the energy producible by 1 square meter of PV panels in a characteristic year. $A_{PV,min}$ corresponds to a design with the highest storage requirements, as all energy that is produced and not instantaneously used must be stored to ensure its use at a later time. By increasing the PV area beyond this theoretical minimum, the energy storage requirements can be reduced.

The energy storage required for 100% output reliability was found by simulating the energy stored over the course of the entire reference year according to Equations (*2*) and (*3*), as plotted in Figure 3. As the PV area is increased beyond the minimum (11 m^2), the battery capacity required to buffer for intermittencies decreases [37]. All points along the curve in Figure 3 (b) correspond to designs with equivalent output in the reference year.

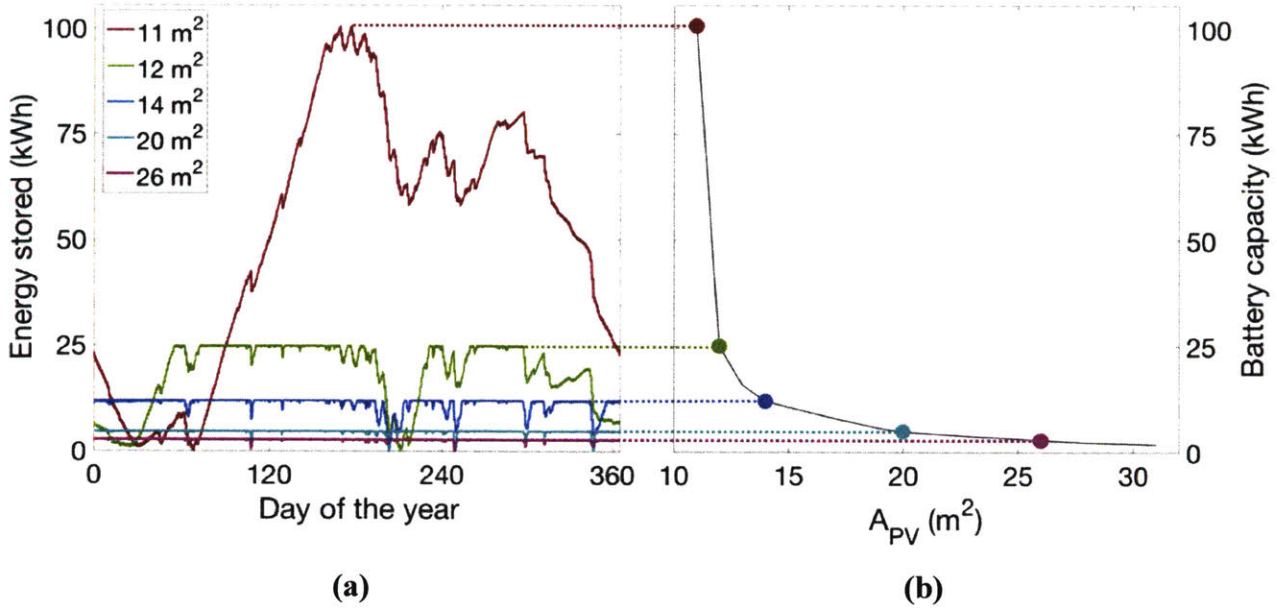

Figure 3. Relationship between PV Area and Battery Capacity

The energy stored for systems with various PV area over the course of the reference year; (b) the battery capacity requirement for each value of PV area. As PV area is increased beyond the minimum acceptable value, the energy storage requirement decreases.

There is a minimum-cost combination of PV panels and batteries that can supply the 8-hour, 1 kW fixed operating schedule reference system. This minimum-cost point lies on the curve represented in Figure 3 (b) and Figure 4, and its value (indicated by the red ring in Figure 4) depends on the ratio of the cost of batteries and the cost of PV. The curve represents a 100% output reliability for the reference year, i.e. production demands are perfectly met given the reference year's solar irradiance data. Alternatively, the curve also represents a loss of power supply probability (LPSP) of 0, where LPSP is defined as the average fraction of time that the load that is not supplied by the PV system [40]. In this analysis, the LPSP is calculated relative to a single reference year, 2014 weather data for Chelluru, India. In the figure, the parallel lines represent constant power system cost (PV plus batteries), where their slope is the ratio of energy storage cost per kWh to PV cost per square meter, and cost increases as the quantity of batteries and PV increases (toward the upper-right corner of the plot). If the ratio of energy storage and PV cost shifts, then the ratio of energy storage and PV area in the lowest-cost design would shift along the

constant output reliability curve. The region above the 100% output reliability curve corresponds to overdesigned power systems which produce more than the required output over the course of the reference year, and the region below the curve corresponds to unreliable systems that do not produce the adequate output throughout the reference year.

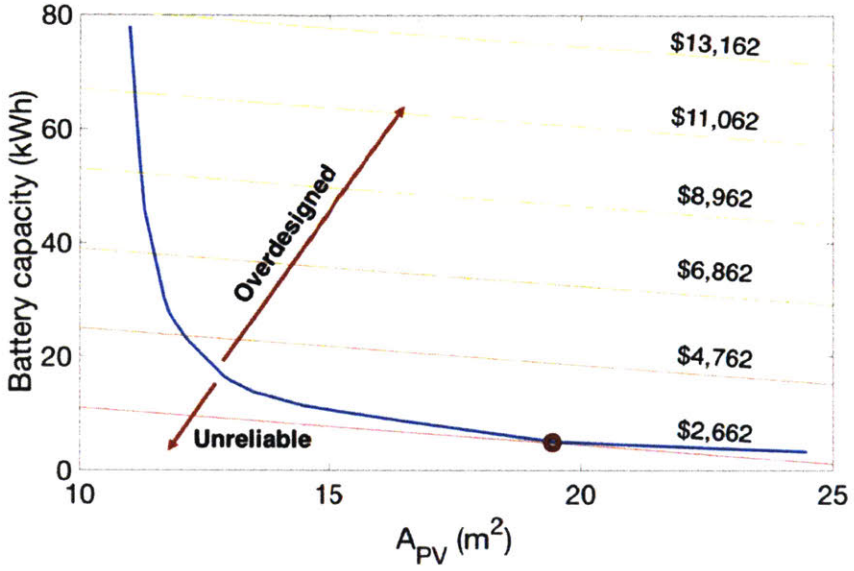

Figure 4. 100% Output Reliability Curve

Locus of power system designs (PV plus batteries) that can provide 100% output reliability in the reference year. Above and to the right of the curve are overdesigned systems which provide excess output, and below and to the left of the curve are designs that do not provide adequate output over the course of the reference year. The diagonal lines represent constant cost power systems, and their slope is determined by the ratio of battery cost to PV panel cost. The lowest intersection point on the locus of power system designs in the direction orthogonal to the constant cost lines corresponds to the lowest-cost power system [37].

2.3 Energy Storage and Product Storage

For processes producing an accumulable output, storage of the output can serve as a secondary storage medium to energy storage in batteries. This can be done when the load is operated on a flexible schedule determined by the solar energy available, as described in the results section. Under certain conditions, utilizing product storage in addition to energy storage can allow

for system cost reductions, as will be described in Chapter 4: Advantages of Operation Flexibility and Load Sizing.

In realistic scenarios, there may also be a volume constraint on the amount of product that can be stored at one time. For example, the village PV-EDR system was constrained to a small plot of land with only enough space for an additional 10 m^3 water storage tank. For this reason, the product storage was constrained to 10 m^3, despite additional cost savings that were possible with a larger water storage tank.

2.4 EDR Behavior

The models used for predicting the performance and behavior of batch electrodialysis systems in this work have been developed and validated by Wright et al. [41] [42]. While it is suggested that the reader review Wright [41], Ortiz [43], Strathmann [44], and Tanaka [45] for a more complete understanding of the electrodialysis process, a brief summary of the general concept is provided here to highlight its relevance to the overall optimization of the PV-EDR system.

2.4.1 EDR Stack Architecture

The EDR subsystem consists of the ED stack, pumps, and water storage and recirculation tanks. The ED stack is composed of cell pairs that are sandwiched between two electrodes, where a cell pair consists of an anion exchange membrane (AEM), a spacer for water flow, a cation exchange membrane (CEM), and another spacer (Figure 5). For this work, the ED stack used was manufactured by GE Water (Model Number AQ3-1-2-50/35). For batch mode, there are two recirculation tanks, for concentrate and diluate respectively, and the water in these tanks is recirculated through the ED stack continuously until the desired salinity is reached. Manual ball valves control the reversal of the streams between batches.

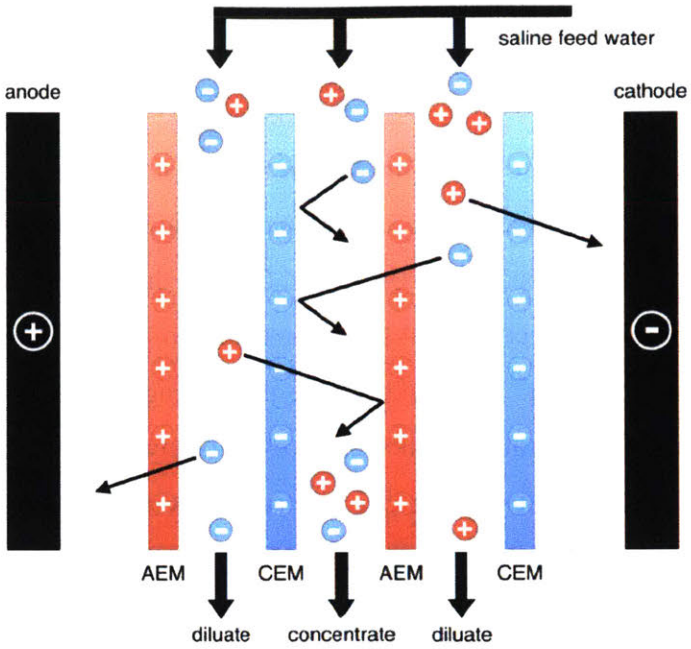

Figure 5. Electrodialysis Process

Electrodialysis separates salts from water through the application of an electric potential across a series of alternating anion and cation exchange membranes (AEM, CEM).

2.4.2 Mass Transfer

The mass transfer of ions from one stream to another was modeled using Ohm's law. The electric potential is the voltage applied across the ED stack, the current is the ion movement, and the resistance is the electrical resistance of the membranes and the streams. Throughout an EDR batch, the current moves ions from the diluate stream into the concentrate stream, producing a concentration profile as shown in Figure 6. Assuming equally-sized and equal numbers of concentrate and diluate channels and assuming perfect mixing, the changes in concentration can be calculated using the mass balance equations (*4*) and (*5*) for the concentrate and diluate streams, respectively (Ortiz 2006):

$$N_k V_k \frac{dC_{conc}}{dt} = Q_{conc} C^0_{conc} - Q_{conc} C_{conc} + \frac{N_{k\varphi} I}{zF} - \frac{N_k A D_a (C^{wa}_{conc} - C^{wa}_{dil})}{l_a} - \frac{N_k A D_c (C^{wc}_{conc} - C^{wc}_{dil})}{l_c}, \quad (4)$$

$$N_k V_k \frac{dC_{dil}}{dt} = Q_{dil} C^0_{dil} - Q_{dil} C_{dil} - \frac{N_k \varphi I}{zF} + \frac{N_k A D_a (C^{wa}_{conc} - C^{wa}_{dil})}{l_a} + \frac{N_k A D_c (C^{wc}_{conc} - C^{wc}_{dil})}{l_c}, \quad (5)$$

where N_k is the number of cell pairs, V_k is the volume of the streams (m^3), C^0_{conc}, C^0_{dil}, C_{conc}, C_{dil} are the concentrations of the concentrate and diluate streams at the inlet and outlet of the electrodialysis stack (mol/m^3) respectively, Q_{conc} and Q_{dil} are the volumetric flow rates (m^3/hour), φ is the current efficiency, I is the current (A), z is the charge of the ion, F is the Faraday constant, A is the active membrane area (m^2), D_a and D_c are the average diffusion coefficients (m^2/s) of NaCl in the anion and cation exchange membranes, respectively, l_a and l_c are the thicknesses (m) of the anion and cation exchange membranes, respectively, t is the time (s), and C^{wa}_{conc}, C^{wa}_{dil}, C^{wc}_{conc}, C^{wc}_{dil} are the concentrations (mol/m^3) on the surface of the anion and cation exchange membranes at the boundaries of the concentrate and diluate streams, respectively. These terms in the equation represent flow of ions at the inlet and outlet of the channels, the ion flow due to the current, and the diffusion of ions across the membranes due to the concentration gradient between the concentrate and diluate streams, respectively.

As the concentrations of the concentrate and diluate streams change, their electrical resistances change. Due to the nonlinear relationship between resistivity and ion concentration, the diluate channels become the dominant resistance in the circuit, increasing electrical resistance overall. During a batch process at constant voltage, this increasing resistance causes a decrease in current over time, slowing the desalination process of removing ions from the diluate stream. This causes the electrical power over the course of a batch to decrease proportionally with the current (Figure 6).

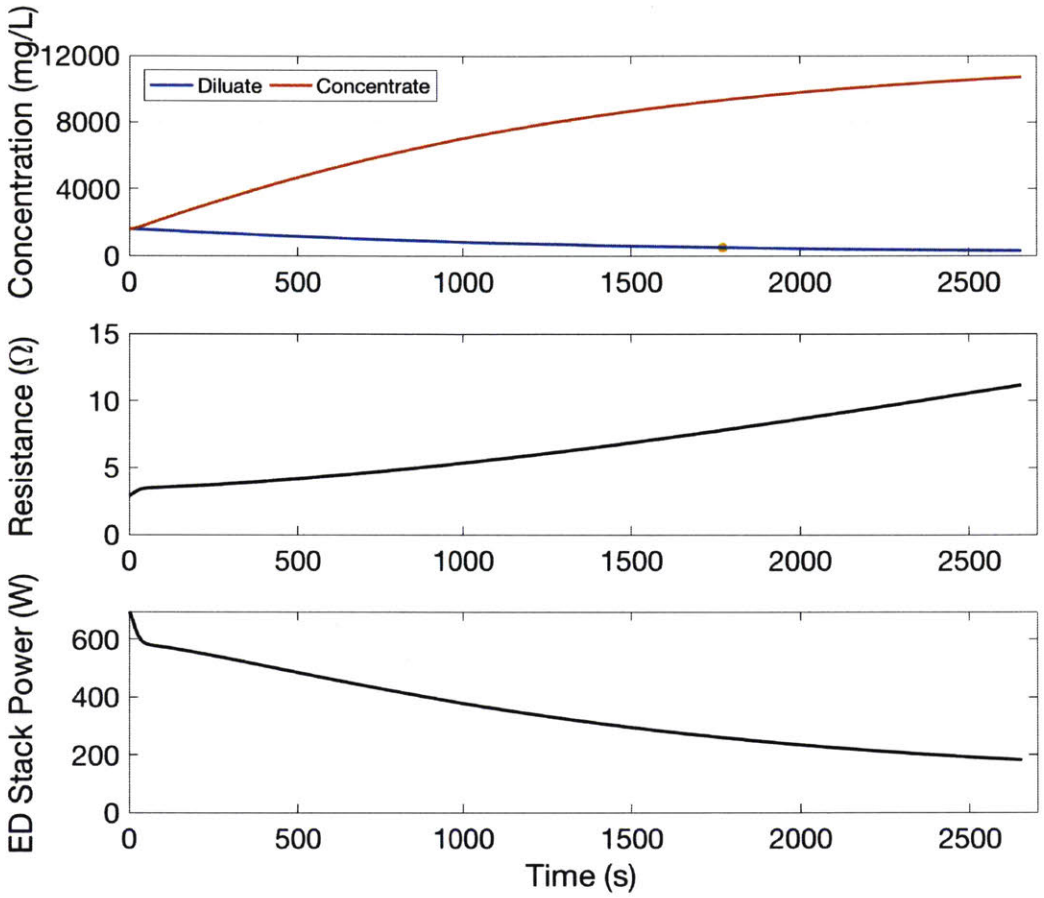

Figure 6: Concentration, Resistance, and Power Over a Single EDR batch.

As the diluate stream becomes less concentrated over the course of a batch, the stack resistance increases, reducing the current and causing the stack power to decrease.

2.4.3 Limiting Current Density

If the applied voltage is too high, then at some point during the batch desalination process the ion concentration at the membrane surfaces in the diluate channels approaches zero. The condition during which this occurs is called limiting current density, which can result in electrolysis of the water molecules, causing harmful production of hydrogen gas and increased pH levels of the desalinated water. The EDR unit should be designed as to avoid reaching limiting current density at any point during the batch process. The limiting current density i_{lim} [A/m^2] is estimated using Equation (*6*),

$$i_{lim} = \frac{C_{dil}^{bulk} zFk}{T_{mem} - t}, \quad (6)$$

where C_{dil}^{bulk} is the concentration of the bulk diluate solution, t is the transport number of the ion in the bulk solution, and T_{mem} is the transport number of the ion in the membrane. The boundary-layer mass transfer coefficient [m/s], k, increases with the linear flow velocity in the channels, causing a proportional increase in the limiting current density. In this analysis, the flow channels, membrane geometry and linear flow velocity are held constant. Holding these factors constant means that the limiting current density varies only with C_{dil}^{bulk}, which decreases over the course of the desalination process, and also that the pressure losses due to flow through the channels are constant.

2.4.4 EDR Design Considerations

For the purposes of this work, we are primarily concerned with desalinated water production rate and power profiles for the entire desalination process, which are the key factors that drive system cost and the value derived by the user. Desalination rate can be varied by changing (1) the applied voltage across the EDR stack and (2) the number of cell pairs, which effectively changes the number of channels and thus the volumetric flow rate, assuming a constant linear velocity through each channel. The range of optimal linear velocities for the spacers in our ED stack was 6-12 cm/s. Because pressure drop per unit length of the spacer exhibits quadratic growth with increasing linear flow rate, we chose to design our system to run at 6 cm/s primarily because it requires less pumping power per unit of flow rate. Additionally, lower linear flow rates are correlated with greater salt removal per unit length of spacer, which is beneficial for effective desalination [46].

The energy and power profiles are also affected by the desalination rate, as increasing the number of cell pairs and the applied voltage requires more power but only produces small differences in the total energy required per volume of clean drinking water. Due to the constant linear flow rate through the channels, the pumping power and energy is proportional to the number

of cell pairs, as the pressure drop remains constant while the total volumetric flow rate increases proportionally with the number of cell pairs.

The applied voltage must be high enough to produce water with the desired TDS level such that 10 m^3 of desalinated water are produced within 24 hours. However, the applied voltage must not be so high that the limiting current density is reached during the desalination process. The maximum number of cell pairs for this study was limited to 170, which is the number of cell pairs available in a fully assembled GE Water ED stack. The recovery ratio, defined as the ratio of diluate water output to feed water input, was chosen to be 90%.

CHAPTER 3

DEVELOPMENT OF A PV-EDR MODEL

A PV-EDR model was developed using the theory of Chapter 2 to demonstrate the application of PV-powered system design principles, to inform the design of cost-minimized PV-EDR systems for any location, and to specifically optimize the off-grid, village-scale PV-EDR system for Chelluru. This model is composed of four modules: the EDR module, the pump module, the power system module, and the cost module. It was designed to take location-specific

parameters and specified values of design variables as inputs, and produce a system capital cost and output reliability for the specific design (Figure 7). When coupled to an optimization routine, the design variable inputs to the PV-EDR model are varied until a design with acceptable output reliability and minimum capital cost is reached.

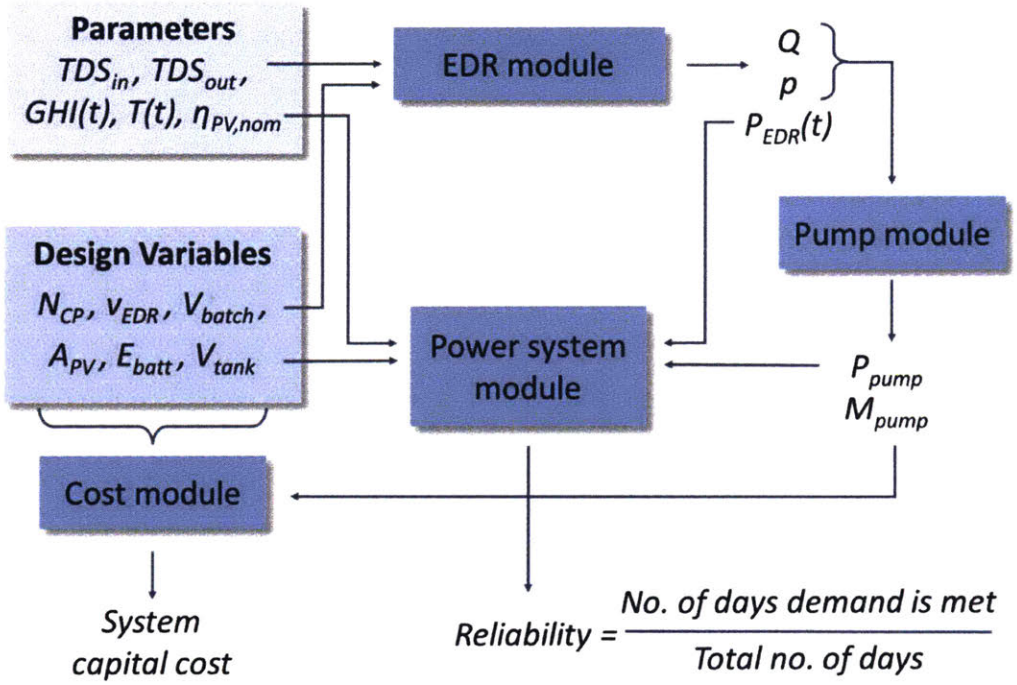

Figure 7. Flowchart of the PV-EDR Simulation

Flowchart of the PV-EDR simulation, where TDS_{in} is the input salinity, TDS_{out} is the output salinity, GHI is the global horizontal irradiance, T is temperature, $\eta_{PV,nom}$ is the nominal PV efficiency, N_{CP} is the number of cell pairs, v_{EDR} is the stack voltage, V_{batch} is the batch volume, A_{PV} is the area of the PV array, E_{batt} is the battery capacity, V_{tank} is the water storage tank volume, Q is the flow rate, p is the pressure, P_{EDR} is the power required for EDR over a batch, P_{pump} is the pumping power, and M_{pump} is the pump model.

3.1 The EDR Module

The EDR module simulates the water desalination process. To do so, it takes the feed water salinity (TDS_{in}), desired output water salinity (TDS_{out}), and desired average daily water production as fixed inputs, and the number of cell pairs (N_{CP}), applied stack voltage (v_{EDR}), and batch size (V_{batch}) as design variables. The module then calculates and outputs the batch time, water desalination rate, power profile (P_{EDR}), the percentage of time that limiting current density was exceeded, and the flow rate and pressure required of the pumps. A design fails in the EDR module if the limiting current density is exceeded, or if the desired salinity of the batch is not reached in sufficient time to allow the daily water production to be achievable.

3.2 The Pump Selection Module

Based on the flow and pressure requirements of the ED system, an optimal pump must be chosen based on cost, ability to provide the necessary flow and pressure, and nominal power draw. A database was created from which to select specific pump models due to a poor correlation between pump performance metrics and cost.

The pump selection module takes the system curve as well as the desired pressure and flow rate of the EDR system as inputs. These are compared to the pump curves of the pumps in the database. The intersection points represent the expected actual operating point of the pump. To evaluate the quality of choice of the pump, the pump selection metric (PSM) of Equation (7) which includes pump cost, power draw, and the difference between the flow rate at the intersection to the desired flow rate was used,

$$PSM = C_{\text{pump}} + 3 \cdot P_{\text{pump}} + 750 \cdot |Q_{\text{desired}} - Q_{\text{actual}}|. \quad (7)$$

The coefficients of each of the comparison metrics of cost, power draw and flow rate difference were chosen to give a cost-like comparison. The cost coefficient is 1 because it serves as a baseline against which the other coefficients are compared. For power, the coefficient is 3 because it is estimated that a small microgrid costs \$3/W [47], allowing a direct addition to the cost metric contribution. Finally, the flow coefficient of 750 was determined through numerical comparison demonstrating that it was sufficiently high such that the flow differential would be

unlikely to exceed 0.1 m^3/hour. The pump in the database with the lowest PSM value for the desired flow rate and pressure is chosen for the design.

3.3 The Power System Module

Solar is an intermittent power source that varies on daily and seasonal scales. A PV-powered system must have the energy storage capacity to provide the required power to the load despite fluctuations on the daily scale (such as clouds and nighttime operation) and variations on the yearly scale, such as lower solar irradiance during the winter season. A combination of PV panels and batteries can meet the power supply profile of an electrical load. The optimal sizing of the PV array and battery pack depends on location-specific weather data, the power profile of the load, and the relative cost of PV and batteries.

The power system module uses time-resolved solar irradiance $GHI(t)$, time resolved temperature data $T(t)$, and nominal PV efficiency $\eta_{\mathrm{PV,nom}}$ as parameter inputs to Equation (*1*) to calculate actual PV efficiency $\eta_{\mathrm{PV}}(t)$. Design-specific values of PV array area (A_{PV}), battery capacity (E_{batt}), and water storage tank volume (V_{tank}), as well as the power profiles of the EDR unit ($P_{\mathrm{EDR}}(t)$) and pump ($P_{\mathrm{pump}}(t)$) are fed into the module. The energy flows into and out of the batteries and the water flows into and out of the water storage tanks are simulated over the reference year period, and an output reliability corresponding to the percentage of days of the year for which water supply meets demand is produced. The simulation will run a batch and charge the batteries according to the logic tree of Figure 8. Within the simulation, the batteries are never allowed to drop below 50%, a value selected to prolong battery lifetime.

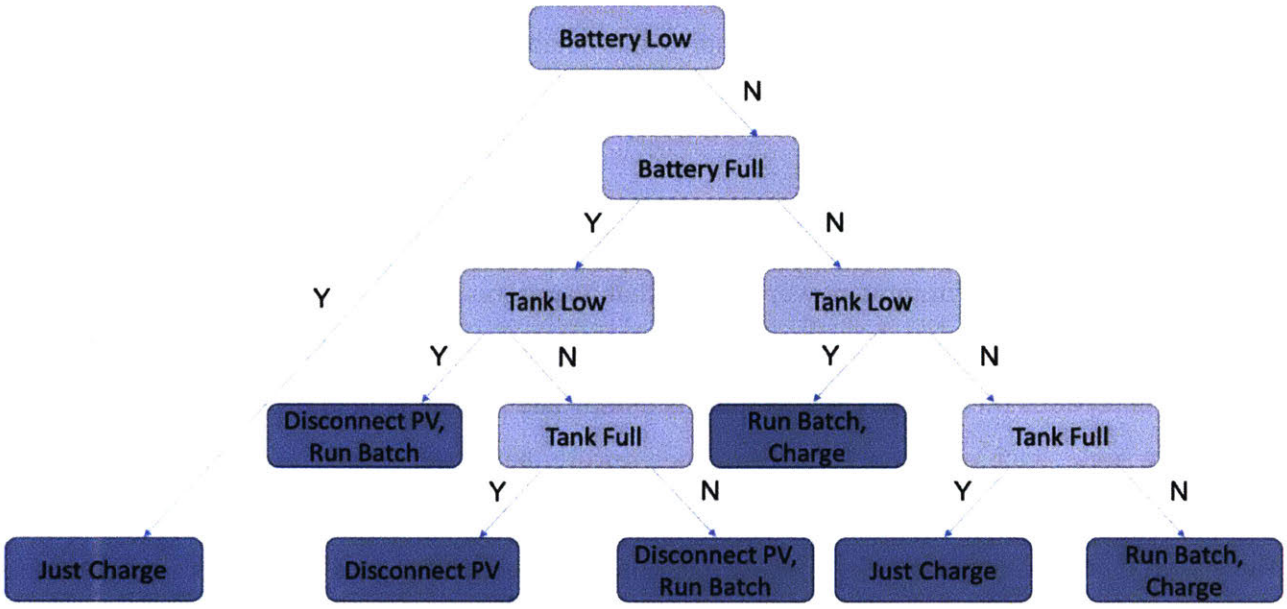

Figure 8. Power System Logic Tree

Logic tree for the power system module, detailing the conditions for charging the batteries and running an EDR batch.

3.4 The Cost Module

The cost module calculates the cost of the PV-EDR system based on the design variables and the selected pump according to Equation (*8*),

$$C_{sys} = C_{PV}A_{PV} + C_{batt}E_{batt} + C_{tank}V_{tank} + C_{CP}N_{CP} + 2C_{elec} + 2C_{pump}, \quad (8)$$

where C_{sys} is the system capital cost; C_{PV}, C_{batt}, C_{tank}, C_{CP}, C_{elec}, and C_{pump}, are the cost of the PV array, battery bank, water storage tank, membrane cell pairs, electrodes, and pumps respectively; and A_{PV} is the area of the PV array, E_{batt} is the battery capacity, V_{tank} is the water storage tank volume, and N_{CP} is the number of membrane cell pairs. An inverter suitable for the optimized power system and EDR and pumping loads is selected retroactively and added to the total system cost.

3.5 PV-EDR Coupled Behavior

Just as the power production of the PV system (energy production and energy storage) can be tuned by the sizing of the panels and batteries, the power consumption of the ED system can be tuned by selecting the quantity of membrane cell pairs, operating voltage, batch size, tank size, and pump model. By jointly adjusting power production and power consumption, the power profiles can be matched in such a way as to optimize the overall system for minimum cost.

Harvested energy can be (1) stored in batteries for later use or (2) used immediately for desalination, storing the excess water in tanks to meet customer demand at times of low or no sunshine. Incorporating water storage tanks as a secondary storage medium to batteries can reduce the energy storage requirement for the system, and a combination of both storage tanks and batteries can enable a minimum-cost design. Due to the coupled nature of the PV and EDR subsystems, it is nontrivial to determine what configuration of the EDR stack, pump models, and quantities of PV panels, batteries, and water storage tanks will result in the lowest capital cost system, and a full-factorial study would be time-consuming and inefficient. Coupling an optimizer algorithm with the PV-EDR performance models can efficiently determine the cost-optimal or near-cost-optimal combination of these components and the accompanying operational specifications for any location.

3.6 PV-EDR Simulation

The performance of a PV-EDR design over a reference year was simulated in Matlab. The input parameters for the simulation (Table 1) are specific to the water quality and needs of Chelluru, and mirror the groundwater salinities and water consumption patterns of a typical Indian village. The solar irradiance and temperature data used for all simulations was obtained from the National Solar Radiation Database (NSRDB) SUNY database for the village of Chelluru, India, in 2014, and interpolated to 5-minute intervals [34]. All references to water production reliability are defined as the percentage of days that the simulation predicted the system would be able to provide the needed quantity of water under the weather conditions of the 2014 reference year. The water collection model assumes 0.25 m^3 of water is collected instantaneously every 15 minutes over the course of 10 hours during the day, resulting in 10 m^3 per day, assuming no seasonal variability. In

future work, measured seasonally-varying demand patterns will serve as input to the simulation for greater accuracy.

Parameter	Symbol	Value
Input TDS	TDS_{in}	1,600 mg/L
Output TDS	TDS_{out}	300 mg/L
Daily water production	V_{prod}	10 m^3
Water production reliability	r_{req}	100%
Solar irradiance	$GHI(t)$	2014 GHI data for Chelluru
Ambient temperature	$T(t)$	2014 data for Chelluru
Nominal PV efficiency	$\eta_{PV,nom}$	15%

Table 1. PV-EDR Input Parameters

Input parameters for the PV-EDR simulation, specific to conditions at the Chelluru test site.

A PV-EDR design was characterized as a combination of the design variables listed in Table 2. The cost of PV, batteries, and water storage were all determined based on local or commonly used component costs. The cost of EDR cell pairs is based on the estimated membrane cost based on supplier quotations for the GE Model Number AQ3-1-2-50/35 ED stack [48].

Design Variable	Symbol	Cost
PV area	A_{PV}	\$98/m^2 [39]
Battery capacity	E_{batt}	\$150/kWh [39]
Water storage volume	V_{tank}	\$110/m^3 [49]
No. of EDR cell pairs	N_{CP}	\$150/cell pair [48]
Stack voltage	v_{EDR}	N/A
Batch size	V_{batch}	N/A
Pump model	M_{pump}	N/A

Table 2. PV-EDR Design Variables

Design variables, the unique combination of which define a PV-EDR system design.

3.7 Optimization

3.7.1 Particle Swarm Optimization

Particle swarm optimization (PSO) is a heuristic optimization approach that iteratively adjusts a population of randomly selected designs (comprised of a defined set of design variables) based on their performance to an objective function [50]. It was selected for this application because of its suitability to searching a complex design space using stochastic methods, and the simplicity of implementation. It was straightforward to couple the PSO algorithm to the PV-EDR simulation.

3.7.2 The Optimized PV-EDR System

PSO was used to determine a cost-optimal PV-EDR design for any given set of parameters and design variables [50]. Due to the stochastic nature of PSO, the optimization converged to a different solution every time it was run. To identify the likely global minimum solution, the optimization was run several times to identify the most promising region of the design space, and was then constrained to exclusively search that narrowed region of the design space to find the cost-minimum design. Table 3 shows the results of the PV-EDR optimization for the Chelluru village system, and the cost breakdown of components is shown in Figure 10.

Design Variable	Symbol	Quantity
PV area	A_{PV}	57.5 m^2
Battery capacity	E_{batt}	22 kWh
Water storage volume	V_{tank}	10 m^3
No. of EDR cell pairs	N_{CP}	62
Stack voltage	v_{EDR}	45 V
Batch size	V_{batch}	0.42 m^3
Pump model	M_{pump}	Kirloskar Wonder III (x2)
Total Cost		**$23,420**

Table 3. Optimized PV-EDR System Design Variables

Summary of design variables for the lowest-cost PV-EDR system found through PSO iteration.

The simulated performance of the optimized PV-EDR design over the reference year is shown in Figure 9. To sustain a long operating lifetime of the batteries, the maximum depth of discharge allowed was set to 50%. During times of low sunshine when the battery was depleted to that level, the water stored in the tank would be used to meet consumer demand, serving as a buffer until the batteries could regain charge. This mode of operation was designed to allow the system to provide the daily water requirement of 10 m^3 either through direct production or by drawing from storage tank reserves.

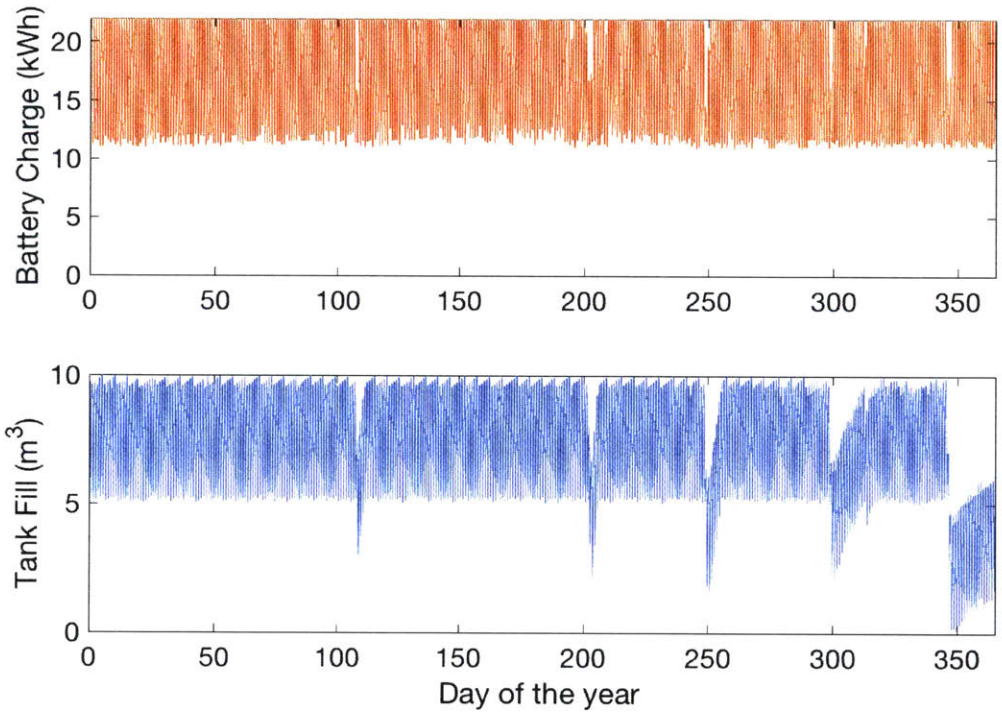

Figure 9. Simulated Battery Charge and Tank Fill Level for the Optimized PV-EDR System

Simulation of the battery charge level and tank fill level for the optimized PV-EDR design during the reference year.

3.8 Comparison to a PV-EDR System Designed Using Conventional Engineering Practices

For comparison, we will call the design in which the optimization of the PV and EDR subsystems was performed jointly Design A. Because village-scale PV-EDR systems are not currently being commercialized, we calculated what a PV-EDR system would cost if designed using conventional methods. This design will be referred to as Design B, in which the EDR system is designed first, and the PV power system is retrofitted to the EDR system based on its power requirements.

For Design B, the EDR system was sized based on two criteria: the daily water production requirement of the median Indian village of 10,000 liters (10 m^3), and an average operation period of 8 hours per day (consistent with the operation period of the on-grid RO system at the test site). Correspondingly, the nominal flow rate of product water was chosen to be 1,250 LPH. The EDR model was used to find the lowest-cost stack (when considered independently from the PV system) capable of producing 10 m^3 per day at a 1,250 LPH production rate. This high production rate requires an approximately 2.5x increase in the number of electrodialysis cell pairs and applied stack voltage compared to Design A (140 cell pairs and a stack voltage of 100 V). However, the number of cell pairs was slightly reduced by increasing the applied voltage per cell pair, resulting in 136 cell pairs and a stack voltage of 98 V. This modification was motivated by the decreased cost of the EDR system. The batch size was selected to be 1 m^3 because it is a commonly-used tank size, and a batch could be desalinated and sent to the water storage tank in less than an hour. A suitable pump was suggested by Tata Projects, our industry partner, based on pumps they commonly use for their water purification systems and their knowledge of the local market. In summary, an EDR stack with a production rate of 1,250 LPH, a 1 m^3 batch size, and 136 cell pairs was selected using this simplified, disaggregated approach. This EDR design had a daily energy requirement, $E_{EDR,d}$, of 20 kWh per day.

To design the power system, a battery capable of providing two days of backup was used, which is a standard metric for sizing PV systems [51]. This resulted in an energy storage requirement of $2 \cdot 20 = 40$ kWh, or 80 kWh assuming a 50% discharge depth. India's average daily global horizontal irradiance solar resource for the region under consideration, $E_{PV,d}$, is 6

kWh/m^2 per day [52]. This average was used to calculate the required area of PV panels according to Equation (*9*),

$$A_{PV} = \frac{E_{EDR,d}}{\eta_{PV} * E_{PV,d}} * 1.3, \quad (9)$$

where 1.3 is a scaling factor to account for losses [53]. In this case, $A_{PV} = 28.9\ m^2$. For water storage, an industry standard 5 m^3 tank is assumed.

The total cost of the PV-EDR system of Design B can be calculated according to Equation (*10*),

$$C_{sys} = C_{PV}A_{PV} + C_{batt}E_{batt} + C_{tank}V_{tank} + C_{CP}N_{CP} + 2C_{elec} + 2C_{pump}, \quad (10)$$

where C_{sys} is the total PV-EDR system cost; C_{PV}, C_{batt}, C_{tank}, C_{CP}, C_{elec}, and C_{pump} are the costs of the PV panels, batteries, water storage tanks, EDR cell pairs, electrodes and the selected pump respectively; and A_{PV}, E_{batt}, V_{tank}, N_{CP}, and N_{elec} are the area of PV panels, amount of battery energy storage, tank volume, number of EDR membrane cell pairs, and number of EDR electrical stages respectively.

The total system cost of Design B was $40,138. The breakdown of cost by system component is shown in Figure 10, from which it is clear that the EDR membranes are the primary contributor to capital cost for Design B. This is because Design B utilized a longer operating time than typical for village-scale desalination systems to achieve a smaller and less expensive EDR stack. The design variables selected through the rule-of-thumb approach for Design B are shown in Table 4.

Design Variable	Symbol	Quantity
PV area	A_{PV}	28.9 m^2
Battery capacity	E_{batt}	62.6 kWh
Water storage volume	V_{tank}	5 m^3
No. of EDR cell pairs	N_{CP}	136
Stack voltage	v_{EDR}	98 V
Batch size	V_{batch}	1 m^3
Pump model	M_{pump}	CNP CHL 2-30 (x2)
Total Cost		**$40,138**

Table 4: Design Variables for Design B Selected Using Conventional Engineering Practices

Design variables for the lowest-cost PV-EDR system designed with conventional approaches.

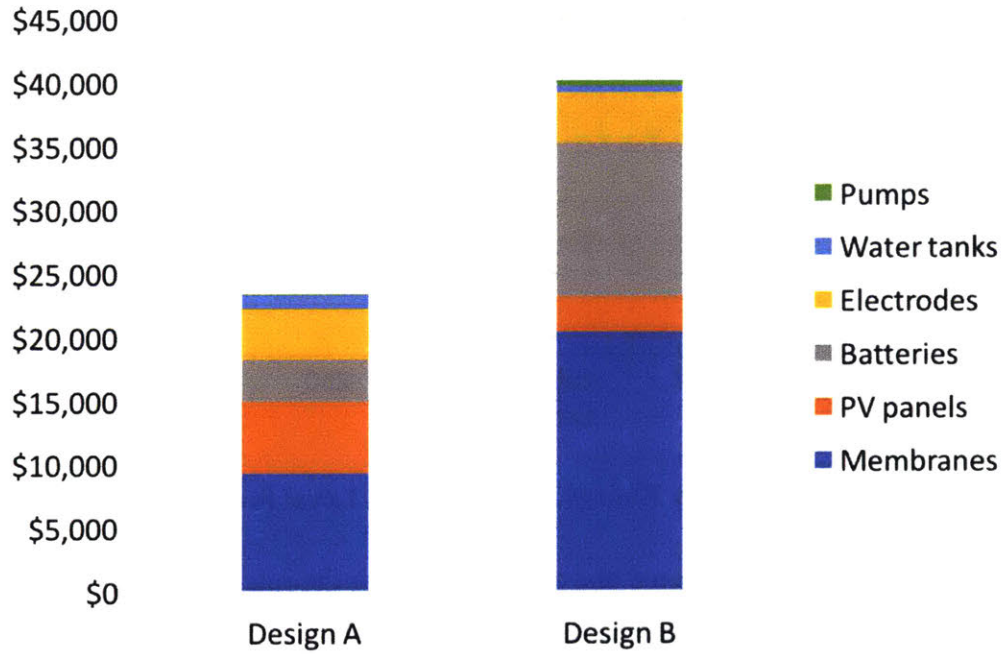

Figure 10: Cost Breakdowns for Design A and Design B

Comparison of cost breakdowns for Design A ($23,420 total) and Design B ($40,138). Design B, designed using rules-of-thumb and a disaggregated approach has a much larger EDR stack which contributes significantly to its capital cost, as well as a larger battery bank; however, it uses a smaller PV array.

A simulation of the performance of Design B over the reference year is shown in Figure 11. It is evident that the battery capacity is highly oversized, such that water storage is at no point utilized for buffering. This also results in the water storage tank being oversized, because the battery is never depleted to its minimum allowable depth of discharge (50%). This shows that in this case, the design rules of thumb produced an oversized PV system for the EDR load.

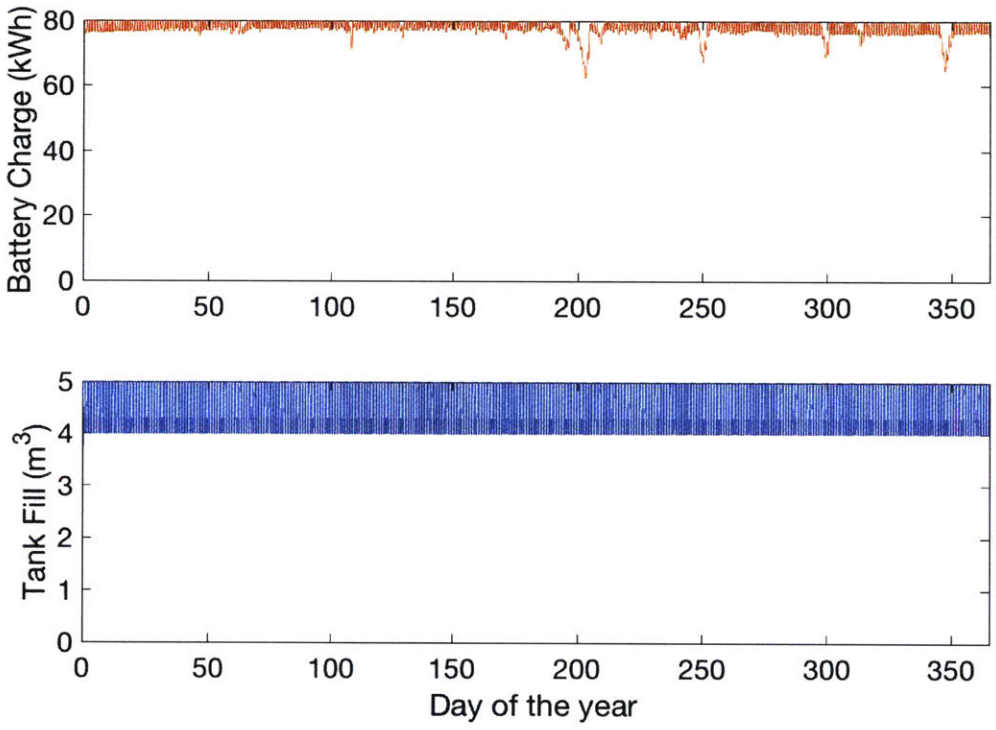

Figure 11: Battery Energy and Tank Fill Level for Design B

Simulation of the battery energy stored and tank fill level for the rule-of-thumb PV-EDR design during the reference year.

3.9 Sensitivities

We used our PV and EDR system models and optimization tools to investigate the parametric relationships between system capital cost, output reliability, and individual component

cost. For each data point, we ran the optimization three or more times to find the associated total system cost value. The relationship between total system capital cost and output reliability is shown in Figure 12. As the output reliability constraint is eased, the capital cost drops sharply, suggesting that just a few days of low sunshine are responsible for an oversize fraction of the system cost. Specifically, a 2% reduction in output reliability (8 days of the year) reduces capital cost by 5.7%, while a 10% reduction in output reliability (37 days of the year) reduces capital cost by 10.3%. The PV-EDR model was designed such that days with a failed water production volume could be penalized by a cost value. If the cost of a failed day of water production is known (for example, the cost to truck in water), that cost can be implemented into the model to find a lower-cost solution. For the village system, we aimed to provide 100% output reliability relative to the reference year, but in future work the flexibility of water sources could be utilized to design an adequate PV-EDR solution at lower cost. Furthermore, inputting actual seasonal water demand into the simulation would illuminate whether the days of lower water production (cloudy, rainy days) coincide with days of lower water demand, reducing the number of failed days. In this analysis, the water demand was assumed constant at 10 m^3 per day year-round due to a lack of any real data.

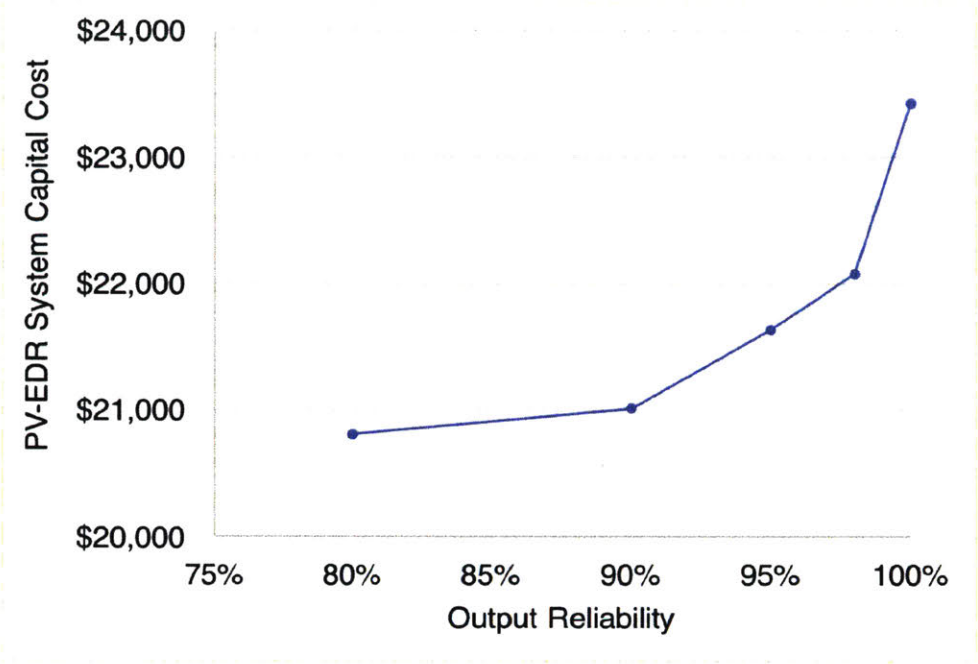

Figure 12. Sensitivity of the PV-EDR System to Output Reliability

Sensitivity analysis of the relationship between output reliability required in the PV-EDR system design (percentage of days of the year for which water production meets demand) and total capital cost. Reducing output reliability from 100% to 98% (8 days of the year where water production is below 10 m^3) reduces capital cost by $1,344, or 5.7%. For 90% output reliability (37 days of the year where water production is below 10 m^3), the capital cost reduction is $2,407, or 10.3%.

The optimization was also run for various reductions in component capital cost for the batteries, PV panels, and EDR membranes. The impact of these component cost reductions on total system capital cost is shown in Figure 13. It is evident that the total system capital cost is most sensitive to the cost of the membranes, relative to the cost of batteries or PV panels.

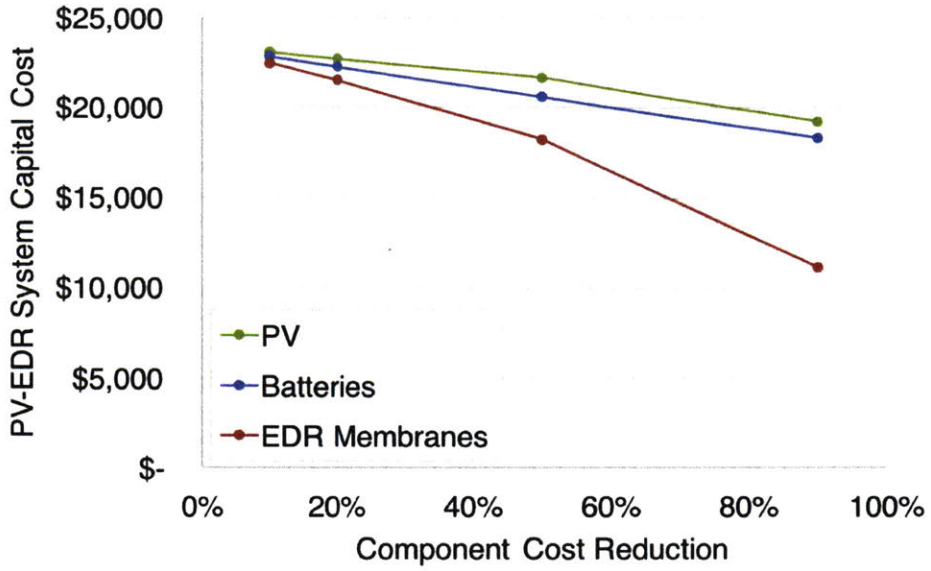

Figure 13. Sensitivity of PV-EDR Capital Cost to Individual Component Costs

Relationship between cost reductions of batteries, PV, and EDR membranes, and total capital cost. For each data point, the cost of all other components is held constant at the current cost values used in the optimal Chelluru system design.

Relative to batteries and PV panels, a reduction in the cost of the EDR membranes would result in the most significant reduction in the total cost of the PV-EDR system. As demonstrated in Figure 10, the membranes are the highest contributor to the cost of the total system. If the membrane cost were to decrease, the EDR stack could be cost-effectively sized larger, and the PV power system could be downsized because of a better overlap of the PV power and EDR power profiles. This effect is described in more detail in Chapter 4.

CHAPTER 4

ADVANTAGES OF OPERATION FLEXIBILITY AND LOAD SIZING

This chapter focuses on two methods for reducing the cost of the PV power system: operation flexibility and load sizing. Operation flexibility is the rescheduling of the operating time of an electrical load to occur during periods of high solar power output. Load sizing is the adjustment of the operating power level and average daily operating duration to better fit the diurnal nature of the solar power profile. Operation flexibility and load sizing are two tools for PV-powered system design that can reduce the size and cost of the PV array and battery bank by shaping the electrical load to better match the time-variant solar power profile.

4.1 Flexible Operation

In Chapter 2, I introduced a theoretical reference system in which a PV subsystem powered a fixed load of 1 kW for 8 hours a day, from 8 am to 4 pm. In this section, I investigate the power system cost reductions enabled by allowing the load operation schedule to shift in time according to the instantaneous solar irradiance available, while maintaining an average operating time of 8 hours per day such that the system produces the same output as it would in a fixed operating schedule scenario. On long days with high solar irradiance, such as during the summer, the system would operate for longer and store the excess product to be collected on a day with low solar irradiance, such that the electrical load would not need to run at that time. Here we assume that product is collected at a uniform rate throughout the year.

To determine the operation schedule that best matched the characteristic solar irradiance for the location, I calculated the highest cutoff value of solar irradiance for which the load should be turned on such that the load is run the same total amount of time over the course of the reference year compared to a load operating on a fixed, 8 hour/day operating schedule. The load profiles for the PV power system for a fixed and flexibly operated electrical load are shown in Figure 14.

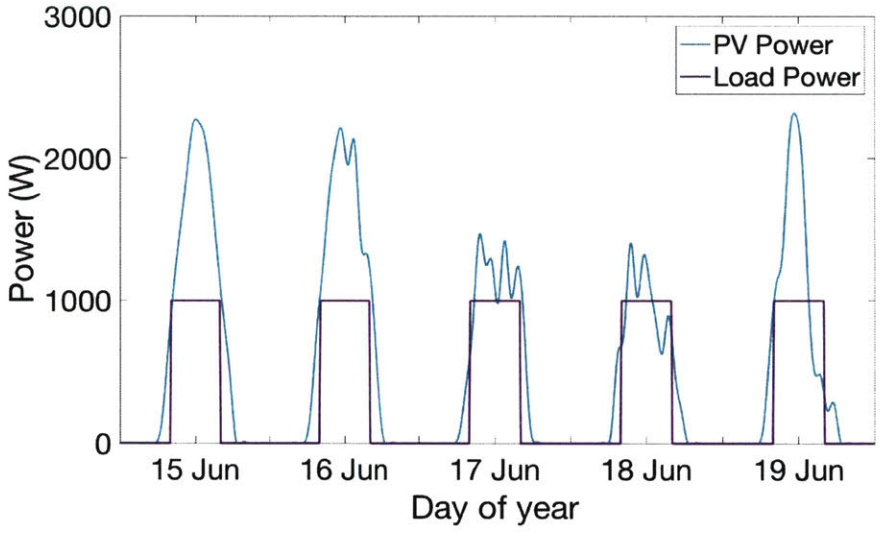

(a)

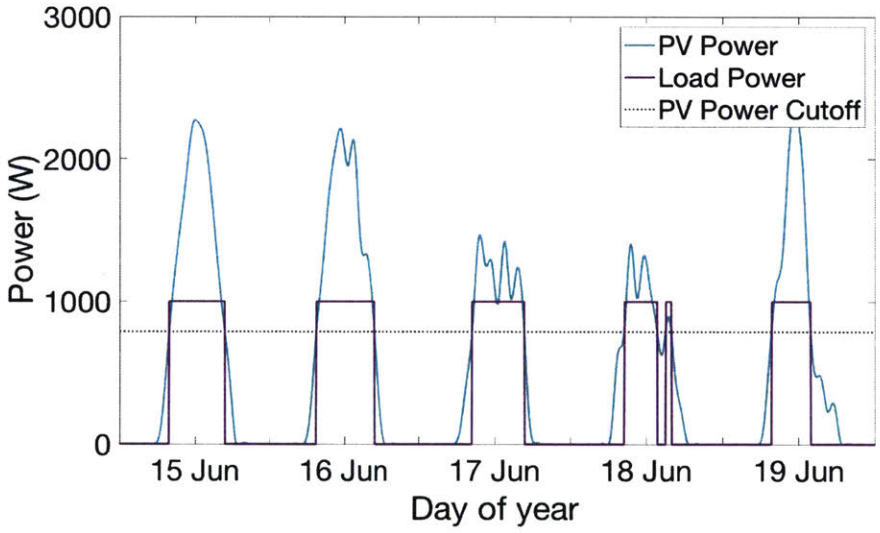

(b)

Figure 14. PV and Load Power Profiles for the Reference System Under Fixed and Flexible Operation

(a) Reference system fixed operating schedule (8am-4pm at 1 kW) load power profile plotted against the power available from the solar power system over 5 days in June 2014; (b) Reference system flexible operating schedule (8 hours daily average at 1 kW) load power profile and PV power cutoff beyond above which the load is turned on.

The advantage of flexible operation is evident in the overlap of the PV power and load power profiles of Figure 14. Flexible operation (Figure 14b) allows for a closer overlap of the power profiles, which translates to a smaller energy storage requirement. The frequency of number of hours operated per day for the reference year using the flexible operation schedule is represented in the histogram of Figure 15. On average, the system operates 8 hours per day, consistent with the fixed-schedule system. However, the spread shows the variability in days of abundant and scarce sunshine. The days with more than 8 hours of operation allow for minimal operation on days with little solar energy available.

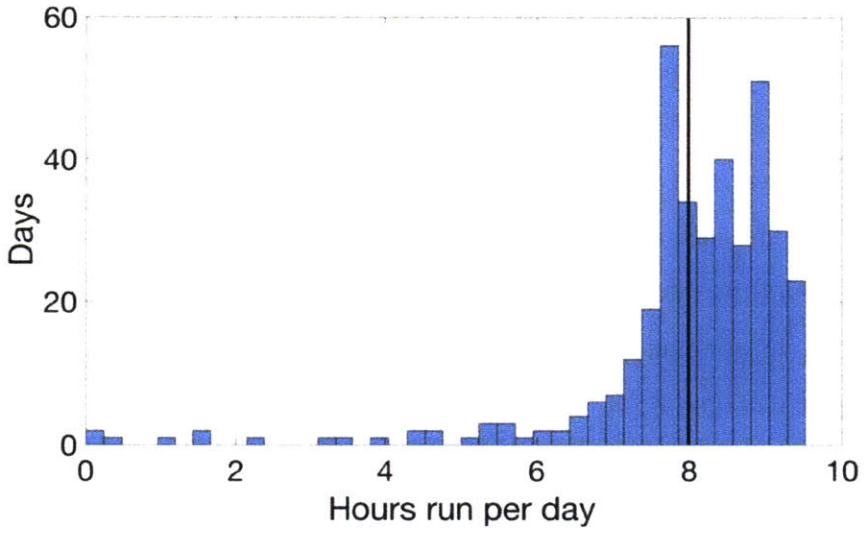

Figure 15. Histogram of Hours Operated per Day for the Flexibly Operated Reference System

Histogram of hours operated per day for the reference system under a flexible operation schedule. The average is 8 hours, equivalent to the fixed operation schedule system, but the spread shows the variability in days of abundant and scarce sunshine. Long operation of 8+ hours on some days of the year allows for minimal operation on the few days of the year for which there is very low PV power output.

The flexibly operated reference system of Figure 15 illustrates the benefits of flexible operation through the spread of hours run per day. Because the system can sometimes be run for 8 to 9.5 hours on very sunny days and store the excess product, the least sunny days of the year can draw from the excess product storage reserves and only operate for 6 or fewer hours per day. For this example, a couple of exceptionally cloudy days of the year would not even need to have the system run at all. This translates to a smaller energy storage requirement, because the system could be turned off and demand could be satisfied by product reserves, rather than large, expensive battery reserves.

4.2 Load Sizing

Load sizing is the adjustment of the operating power and average duration of the load to better match the solar power profile. Certain processes, such as drip irrigation and municipal water supply, require a roughly constant energy to produce a set output over a day, but the sizing of the unit and the power at which it operates can be flexible over a range. The pumping system for irrigation or supplying a water tower, for example, could operate at high flow rate for a shorter period of time, or a low flow rate for a longer period of time. Here, the flexibly-operated reference system described above operates on average 8 hours per day, at 1 kW. Alternatively, another system of half the size can operate at 0.5 kW and produce the same output in 16 hours. Or, another system twice the size of the original can operate at 2 kW and produce the desired output in 4 hours. In each case, the energy used to run the system is the same, at an average 8 kWh per day.

A representation of the load power profile and PV power output for a PV-powered system is shown in Figure 16. Load sizing is the adjustment of the load power profile to overlap with the typical PV power profile. In this analysis, I compare loads with different profiles but equivalent energy consumption (the area under the load power curve is kept constant).

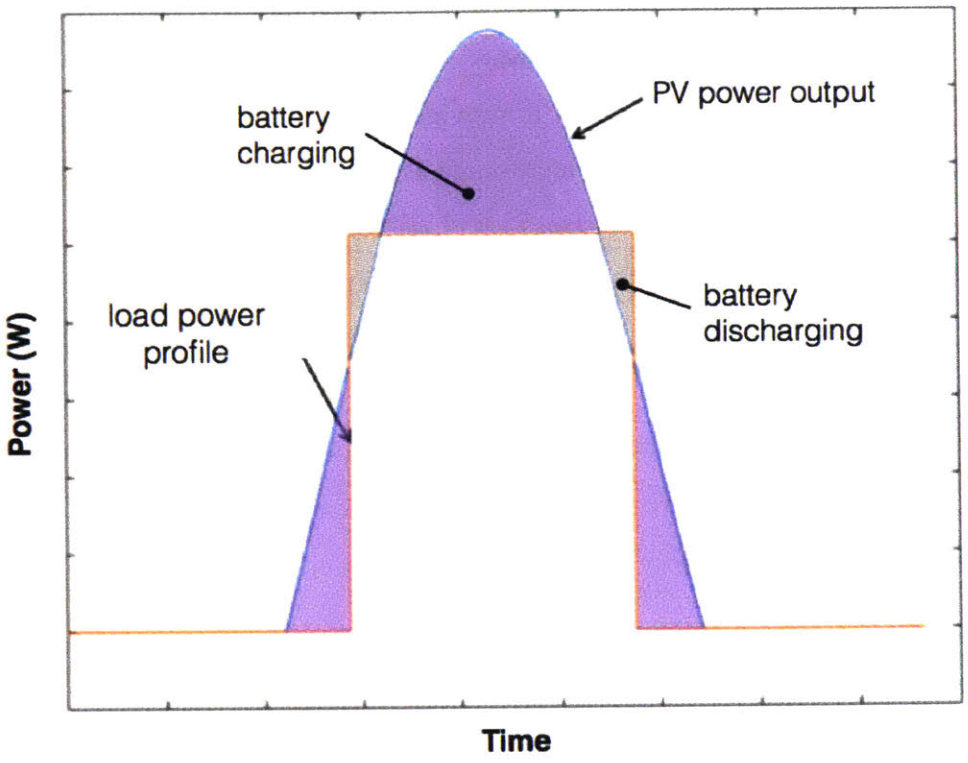

Figure 16. Illustration of a Load Power Profile and PV Power Output

The overlaid load power profile and PV power profiles for a theoretical PV-powered system. Load sizing is the adjustment of the load power profile to better fit the characteristic PV profile, by adjusting the power level and duration of operating time.

4.3 Effects of Operation Flexibility and Load Sizing on the Reference System

The flexible operation schedule improves the overlap of the load power and PV power profiles. The storage requirement associated with variable PV area is shown in Figure 17. For the same size PV array, the required energy storage is lower for the flexible operation case. Flexible operation also pushes the design toward a smaller PV array. However, the flexibly-operated design requires additional product storage for 100% output reliability, the cost of which is not included in Figure 17 (b). Depending on the cost of product storage, flexible operation may be more or less favorable than fixed operation. In the flexible operation mode (Figure 14 (b) and Figure 17),

flexibility was maximized such that energy storage was minimized, and resultantly, product storage was maximized. This means that 82 hours' worth of product needed to be stored to balance the fluctuations in annual solar availability to provide 100% output reliability. Flexible operation is cost-effective when the cost of product storage is less than the power system cost savings afforded by flexible operation—in this case, $1,034. This analysis assumes a constant demand for the output throughout the annual cycle. If demand for output tracks with higher solar irradiance, the product storage requirements and associated costs would be reduced, and flexible operation would become more cost-effective. This effect is expected with a product like desalinated drinking water, which would have a higher demand during sunnier, hotter times of the year.

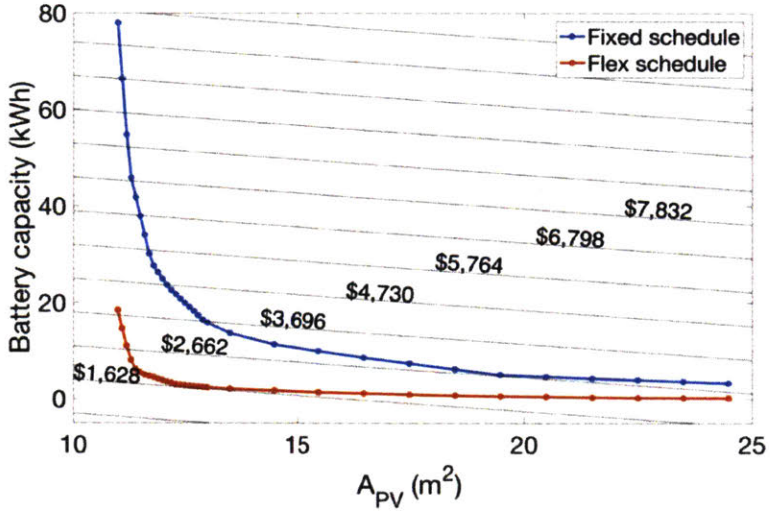

(a)

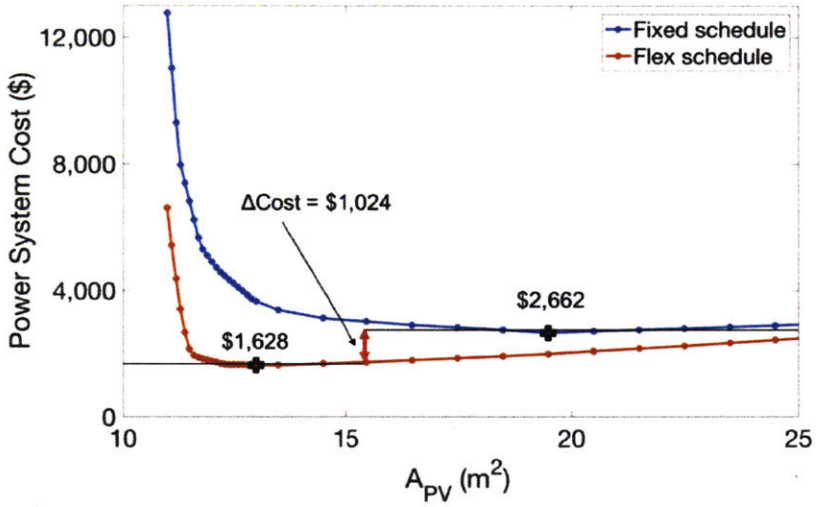

(b)

Figure 17. Relationship Between PV Area, Battery Capacity, and Power System Cost for Fixed and Flexible Operation of the Reference System

(a) The relationship between PV array size and storage requirement (represented here as battery capacity) for the reference system operating according to fixed and flexible schedules. The diagonal lines represent lines of constant power system cost, increasing upwards, and are determined by the ratio of energy storage and PV cost. (b) The relationship between PV array size and total power system cost (PV + batteries) for both fixed and flexible schedule designs. The black markers indicate the points of lowest power system cost ($2,662 for fixed operation and $1,628 for flexible operation).

To determine the effect of load sizing on power system cost, I calculated the lowest-cost combination of PV panels and batteries to meet the load power requirements for different load power profiles. For each load power profile, I held energy consumption constant, but adjusted the constant power level and duration of operating time. The cost of the power system for designs with different lengths of average daily operating time (but equivalent energy consumption per unit output) are plotted in Figure 18.

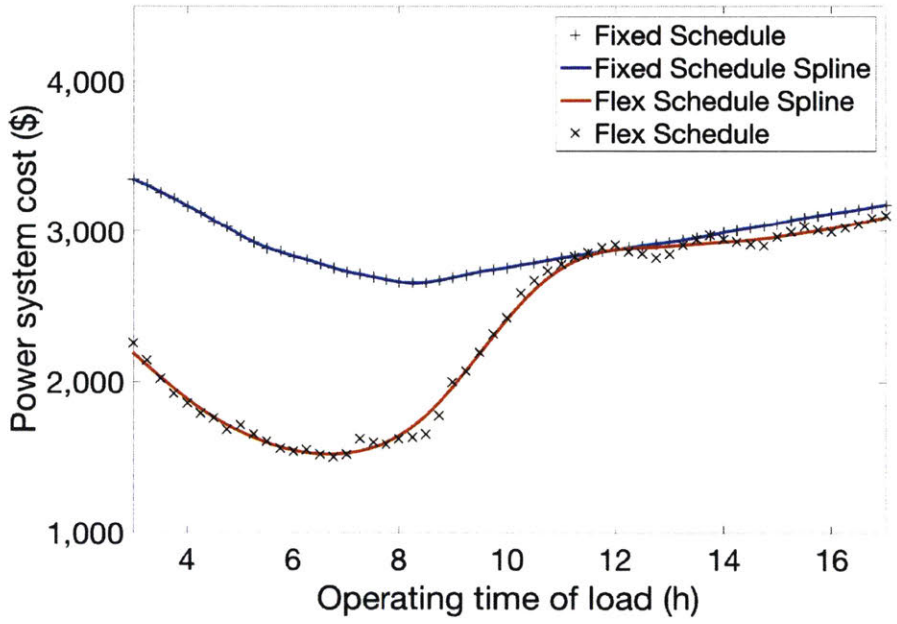

Figure 18. Power System Cost for the Reference System for Various Load Sizing

Lowest-cost power system (PV plus batteries) for a flexibly-operated reference system with varying daily operating time/power levels. Each design consumes an average of 8 kWh per day, but the power at which it operates and the corresponding number of hours it runs per day varies along the *x*-axis. The flexible-schedule systems have a lower cost than the fixed-schedule systems up to a 12-hour daily operating time, at which point flexible operation does not provide value because the system must always run at some point when there is no sunshine available.

The flexible operating schedule provides the greatest cost reductions around an average daily operating time of 5 to 8 hours, or corresponding power levels of 1 to 1.6 kW. This enables a power system cost reduction of 43% compared to a fixed-schedule system. It is important to note

that higher-power electrical loads tend to have a higher capital cost than smaller, low-power loads, so there is a competing effect on the optimal electrical load size that may push the operating time to longer hours when the capital cost of the electrical load is considered. For example, if the capital cost of the electrical load is $4,000 for 0.5 kW, 16-hour operation, and $8,000 for 1 kW, 8-hour operation, the summed capital costs of the power system and electrical load would be $6,999 and $9,624, respectively. Because the capital cost of the electrical load is so high relative to the cost of the power system, the 0.5 kW/16-hour design is more cost-effective. Additionally, the flexible schedule system requires more product storage than the fixed schedule design, which may reduce the relative cost advantage of flexible operation depending on how much product storage costs.

4.4 Effects of Operation Flexibility and Load Sizing on the PV-EDR System

As discussed in Chapter 3, the optimized PV-EDR system had an average operating time of 17:42 hours per day. Desalination rate is proportional to the number of EDR membrane cell pairs that make up the EDR unit. To produce the necessary 10,000 liters of product water per day, the optimized PV-EDR system was required to operate for this duration. Figure 19 illustrates the frequency of number of hours operated per day for the optimized PV-EDR system. Aside from several outliers, the system was expected to run 17:42 hours every day. The optimization converged on this design with a long operation schedule because it allowed for a smaller EDR unit, which was favorable due to the very high current capital cost of EDR membranes ($150/cell pair). Because of the dominance of membrane cost in the optimization, this PV-EDR system design could not take advantage of the power system cost reductions afforded by operation flexibility.

However, it is not unreasonable to assume that ED membrane costs will drop significantly compared to the current cost of the membranes used in the GE EDR stack. According to manufacturer quotations from Iontech, a company producing electrodialysis systems, their membranes cost $40 per m^2 [54]. Electrodialysis membranes are a small market right now and their cost is expected to drop further if economies of scale are achieved. To investigate the effect of significant, but reasonable reductions in membrane cost, we performed the PV-EDR optimization using a membrane cell pair cost of $20. The optimized PV-EDR design with the reduced membrane cost of $20 per cell pair is shown in Table 5. Because of the reduced capital

cost of the EDR unit, the daily operating time for this design is 8:35 hours, which allows operation in the flexible regime. A comparison of the hours operated per day for the EDR system optimized for $150 cell pairs and the system optimized for $20 cell pairs is shown in Figure 19. The $20 per cell pair design has a larger EDR stack enabled by the lower cost of membranes, and a correspondingly shorter average operating time and higher peak power. Its power profile is better matched to the solar power profile, which allows for a downsized PV array and battery bank.

Design Variable	Symbol	Cost	Quantity
PV area	A_{PV}	\$98/m^2	31 m^2
Battery capacity	E_{batt}	\$150/kWh	5 kWh
Water storage volume	V_{tank}	\$110/m^3	10 m^3
No. of EDR cell pairs	N_{CP}	\$20/cell pair	133
No. of electrodes	N_{elec}	\$2,000/electrode	2
Stack voltage	v_{EDR}	N/A	95 V
Batch size	V_{batch}	N/A	0.68 m^3
Desalination rate	r_{desal}	N/A	1224 LPH
Daily operating time	t_{op}	N/A	8:35 h
Peak power	P_{pk}	N/A	2,360 W
Total Cost		**\$11,717**	

Table 5. Optimized PV-EDR Design with $20 Membrane Cell Pairs

Cost and quantity of components in an optimized PV-EDR design, where membrane cost was reduced from $150 to $20 per cell pair. The total optimized system cost was $11,717. This represents a power system cost reduction (PV and batteries) of 57.5% compared to the 17:42 hours/day PV-EDR design.

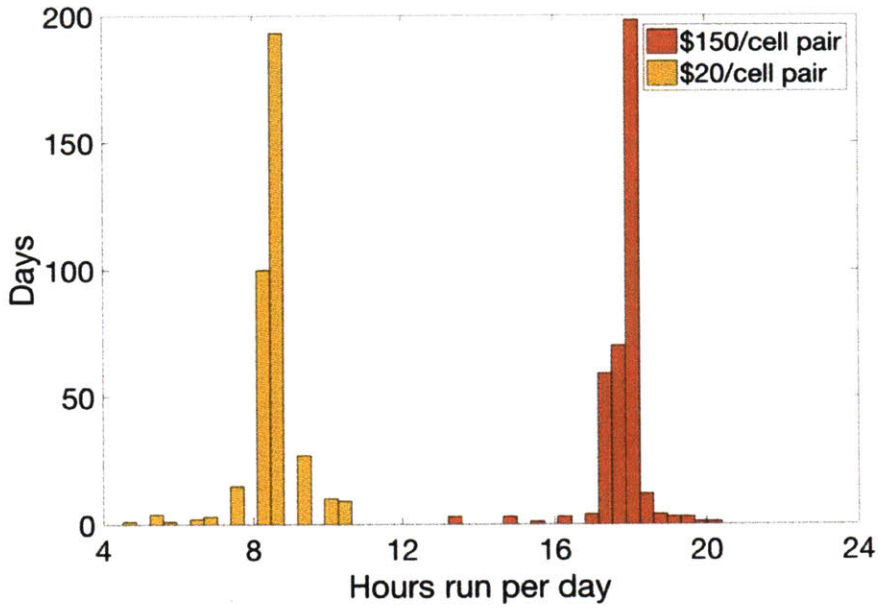

Figure 19. Hours Operated per Day for $20 and $150 Membrane Cell Pair Systems

Histograms of the EDR system designed to run on average 8:35 hours per day ($20 cell pairs) and 17:42 hours per day ($150 cell pairs).

When the capital cost of the electrical load is comparable to the cost of the PV power system, as was the case with the $20 membrane cell pair system, there are dramatic reductions in the power system cost, and the PV-EDR system cost overall. This finding is consistent with the high sensitivity of total system capital cost to the cost of the membranes described in Chapter 3, and motivates the development of lower-cost membranes, both through innovation and economies of scale.

CHAPTER 5

DESIGN AND FIELD TESTING OF A PV-EDR SYSTEM

5.1 Experimental Setup

To collect real-time weather data to feed into the models to validate the field pilot test, a weather station was installed in the Tata Projects Water Development Center near Hyderabad,

India. A Campbell Scientific LI200RX pyranometer was used to measure solar irradiance, and a HC2S3 temperature and relative humidity probe was used to measure the ambient temperature.

The PV-EDR system was installed alongside an existing grid-connected RO system in Chelluru. The PV array was installed on the rooftop while the EDR system, pumps, batteries and inverter were installed inside the small building housing the RO system. The inverter model was the UTL Alfa PCU, which is capable of measuring and exporting time-resolved data related to the PV power, battery status and load capacity. The full PV-EDR system was assembled as detailed in Figure 20. The experimental system deviated from the optimized system described in the previous section in the following ways:

1. An error in the model used to design the experimental system: After design and installation of the Chelluru EDR system, an error was discovered in the power system code that miscalculated the energy used by EDR during a battery discharging state. This was because Equation 2 was used to calculate the energy flows for charging *and* discharging, so the 85% battery efficiency was multiplied against the energy flowing from the batteries, resulting in a smaller discharge than there should have been. This error caused the Chelluru system to be undersized, so that it was only capable of producing 7 m^3 of water per day rather than the expected 10 m^3. This error was corrected in the analyses presented in this thesis, but is a primary cause for the lower water production rates observed during village testing.
2. The composition of the experimental system varied in some respects to the optimized system due to practical constraints and limitations of what was actually available locally:
    a. The battery bank used in the experimental system was 16.2 kWh (utilizing a discharge depth of 50%), as opposed to 15.5 kWh selected initially by the optimization due to the error in the code described in point 1. To supply at least 15.5 kWh, 10 12V batteries of 1.62 kWh storage were connected to supply 120V to the inverter. This battery capacity is lower than the 21 kWh of energy storage selected by the corrected optimization.
    b. The GE ED stack was originally a two electrical stage unit, and was modified to only use one electrical stage (2 electrodes, rather than 4). This required rerouting the water streams within the first electrical stage which was not electrified. Only the electrodes associated with the electrified stage were counted toward the pilot system capital cost,

but because of the construction of the unit, the first electrical stage could not be removed.

c. The Kirloskar Wonder III pumps selected by the optimization were not corrosion-resistant, so Grundfos CM 3-3 pumps with similar flow and pressure characteristics and corrosion-resistant construction were substituted. These pumps cost $239 each, $195 more than the pumps originally selected through the optimization.

d. The installed system used a UTL Alfa PCU inverter which was selected retroactively, and the cost of which was not considered in the optimization.

e. Additionally, the installed system used a power supply to provide DC voltage to the EDR stack from the AC inverter.

3. Operation of the PV-EDR system during the testing period was different from the simulated operation in the following ways:

   a. The simulation used to design the village PV-EDR system did not consider the recirculation tank filling and draining time and associated pumping power. The filling and draining added approximately 15 minutes to each batch, during which time one 410 W pump was running.

   b. Because the PV-EDR system was manually operated, there was some variation in batch length from what was represented in the model.

   c. Halfway through the 7-day test, significant scaling was observed within the EDR stack because of precipitation of dissolved salts in the concentrate stream. To alleviate this, the recovery ratio was reduced from 90% to 80%.

4. The Chelluru PV-EDR system, and any other realistic system, has several components that were not considered in the optimization but add to the total capital cost. These are recirculation tanks, piping, valves, PV racking and wiring, and pre-filters.

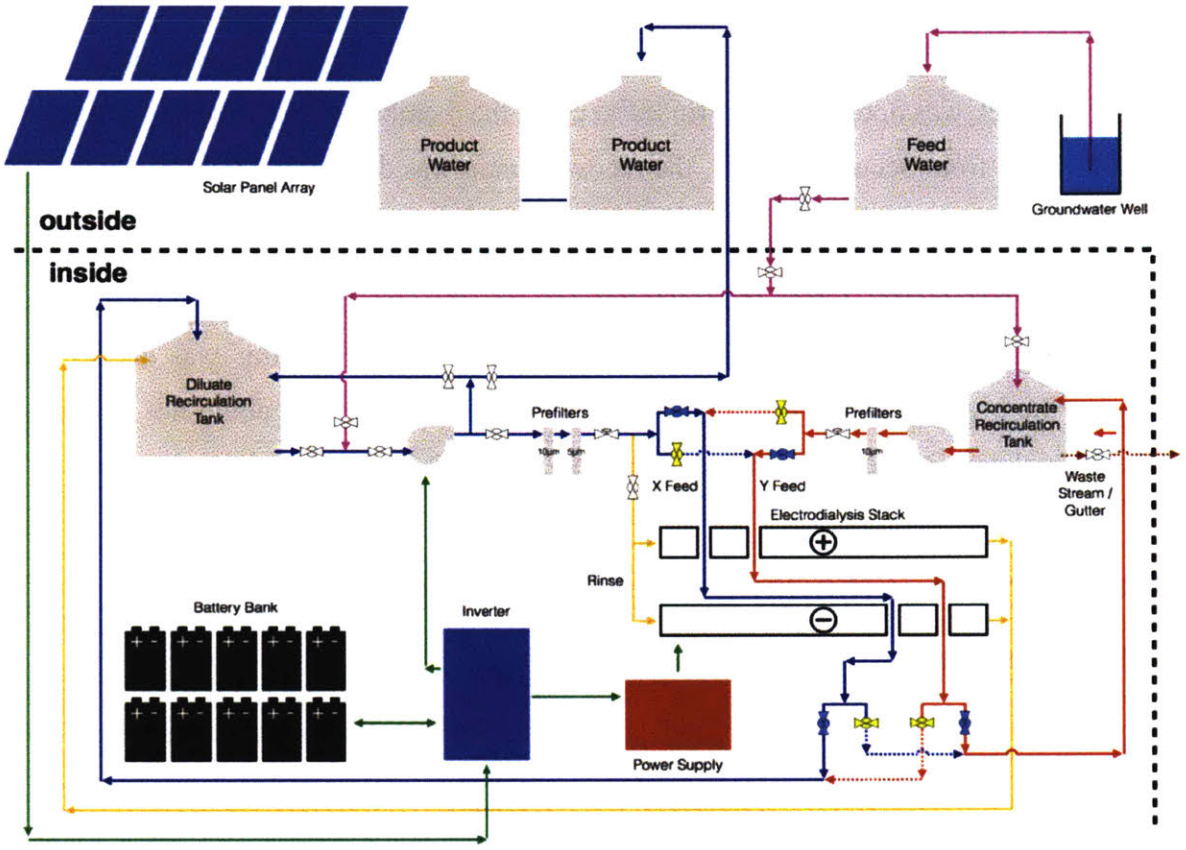

Figure 20. Layout of the Pilot PV-EDR System

Layout of the pilot PV-EDR system installed in Chelluru.

5.2 Experimental Procedure

The PV-EDR system was run in the village from early evening on April 19 to early evening on April 26, 2017, for a total period of 7 days. A single EDR batch was comprised of a complete cycle of filling the recirculation tanks, desalinating the water, and emptying the recirculation tanks. The filling phase consisted of pumping water from the feed water storage tank to fill the diluate and brine recirculation tanks; the desalinating phase consisted of circulating the water through the ED stack while applying the desired voltage until the average salinity in the diluate tank was measured to be 300 mg/L or less; and the emptying phase consisted of draining the brine water into the village gutter and pumping the diluate water into product water holding tanks.

During testing on April 23, we discovered that scale formations had been accumulating over the course of the first few days of testing. There was a 23-hour gap between batches during which the ED stack was opened up and rinsed to clean the membranes of the scale formations. To prevent this issue from occurring again, the recovery ratio was decreased to approximately 80%, effectively doubling the size of the brine volume per batch.

Another irregularity during the weeklong test was the presence of several gaps in the data recorded by the inverter, from minutes to hours at a time. We expect this was due to a faulty condition in the inverter datalogging process. Because this missing data could not be recovered, there are several gaps in the experimental data presented in the following sections.

5.3 Comparison of the Modeled and Measured Performance

5.3.1 EDR Load Power

At the Chelluru test site, the load power was measured through the inverter, and the pumping power was verified by measuring the AC current to each pump with a multimeter. The power profiles of filling and emptying the recirculation tanks before and after each batch respectively were added into the model. In order to compare the power profile during the desalination phase, the simulated power draw during that period was plotted against the average experimental power draw and the range of a single standard deviation for 46 batches (Figure 21). On average, the experimental power draw profile exceeded the simulated power draw profile during the first half of the batch and dropped below by the end of the batch. The model predicted the magnitude of the EDR load within 13.5%, and closely matched the expected batch duration of 60 minutes.

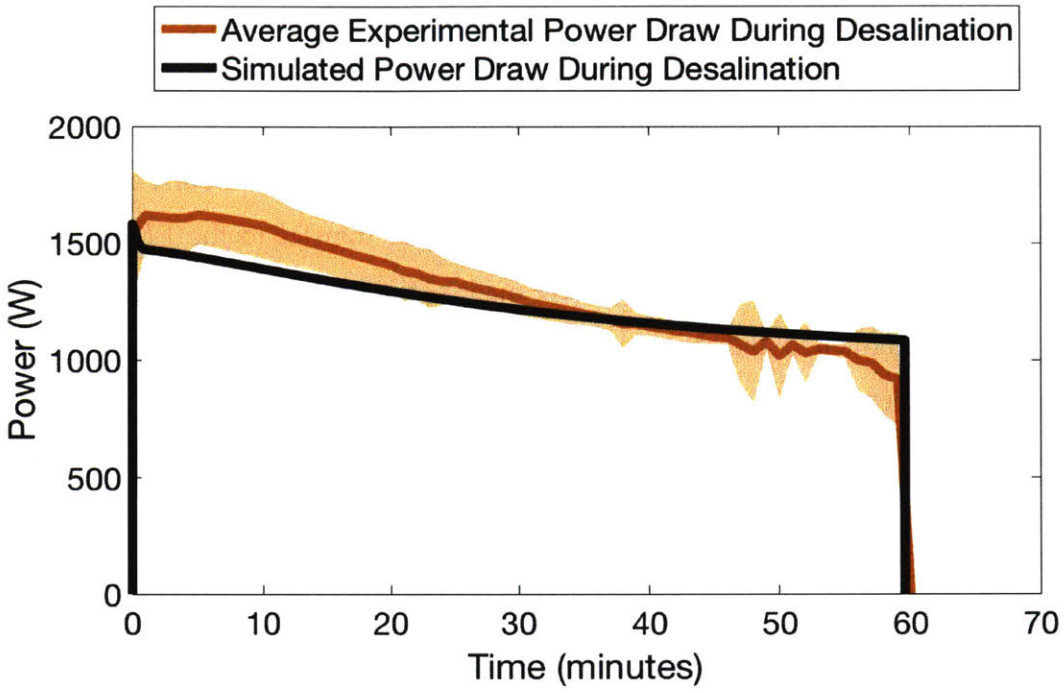

Figure 21: Comparison of Simulated and Measured EDR Power Profiles

Simulated power draw profile during the desalination phase of a single batch (black) compared to the average experimental batch (orange) with 1 standard deviation (shaded region).

While the average desalination phase duration was 60 minutes, it varied from 32 to 115 minutes at the extremes, although most were within the 45-80 minute range. The longest duration batches occurred when there was heavy scaling on the membranes, as the flow rate decreased dramatically as the stack became clogged with salt. While there was some variation in batch volume during testing, these differences do not fully account for the full range of batch durations that were observed.

A comparison of the modeled and measured power profiles over the course of a single day (April 20, 2017) are plotted in Figure 22. The modeled power profiles consist of 20 minutes of draining and refilling the recirculation tanks with one 410 W pump on, followed by a 60 minute-long EDR batch with two 410 W pumps running and the voltage applied across the stack, decreasing in power over time. Due to the data collection failures, data from a number of the batches that were run are missing, including 2 batches in the morning of April 20.

The power load measured by the inverter during the desalination phase was higher than anticipated through the model, particularly at the beginning of each batch, though the match was closer near the end of each batch. Figure 22 shows the inverter-measured load power over the course of a single day of testing plotted against the simulated power profile. Because the pumping power measured by the inverter was validated by separately measuring the current to the pumps, we expect that the discrepancy lies somewhere in the power transfer to the ED stack. Manual measurements of the stack voltage and current were made periodically throughout several batches. These measurements indicated that the actual power consumption according to the manual measurements was in better agreement with the model than the data collected from the inverter. This may indicate that the power supply used to supply the DC voltage to the EDR stack had a substantially lower efficiency at high power outputs than at lower power outputs. This would explain why the modeled and measured values differ greatly at the beginning of a batch but converge at the end.

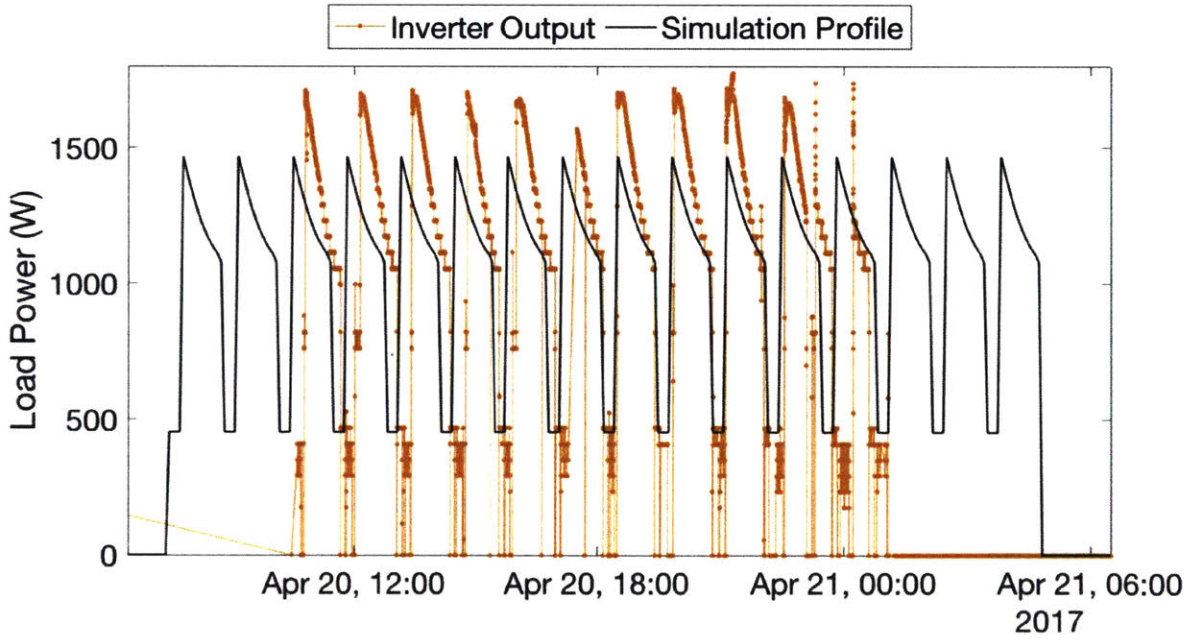

Figure 22. EDR Load Power

Comparison of the power output data collected from the inverter in April 2017 (orange) and the expected power profile based on the simulation model over the course of 2014 (black).

5.3.2 PV Panel Output

The solar power produced by the PV array was measured at the Chelluru test site through the UTL Alfa PCU inverter, and the solar irradiance was measured at the Tata Projects Water Development Center manufacturing facility (approximately 60 km west of Chelluru) and used to calculate a modeled PV power output based on the 40 m^2 of panels of the pilot system according to the method described in the PV Power System Behavior section. A comparison of the modeled PV array power output (using the measured 2017 weather data), the PV power output used in our simulation to design the system (based on semi-empirical 2014 weather data), and the measured PV power output from the pilot system inverter is shown in Figure 23.

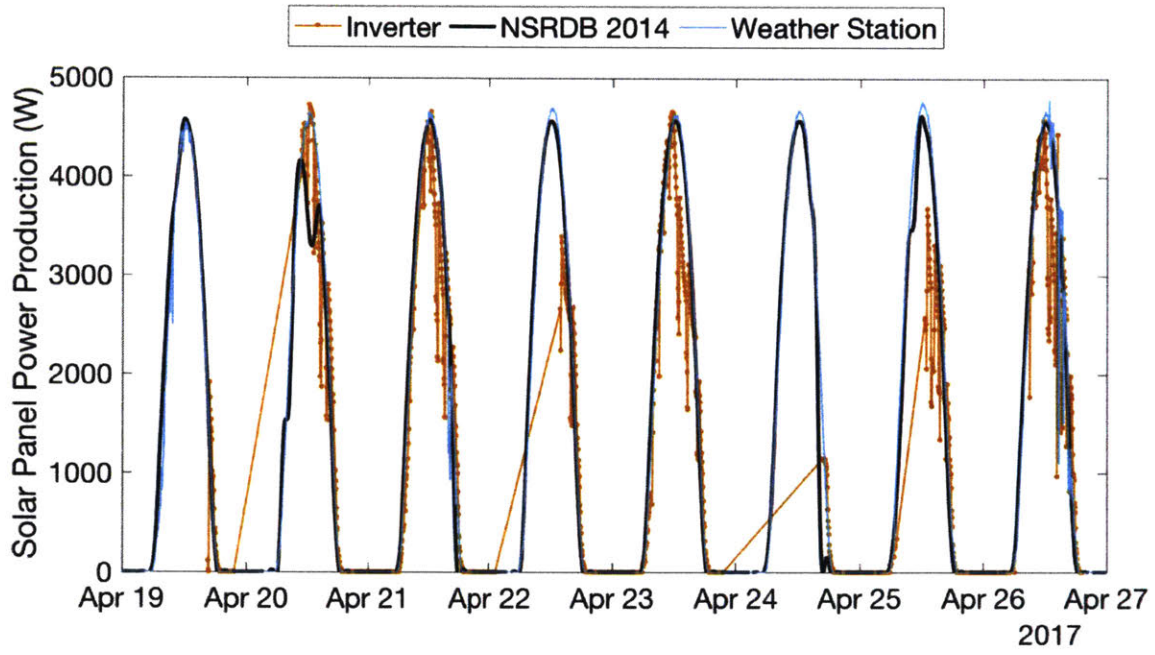

Figure 23. PV Array Power Output

Comparison of the solar panel power production data collected from the inverter in April 2017 (orange), the simulation model based on the NSRDB 2014 weather data (black), and the model prediction using the weather data collected from the installed weather station (light blue).

The 2014 semi-empirical data and the measured 2017 data from the weather station are very similar. Though it is not an indication of long-term agreement, this indicates that the simulation results using the 2014 data should be similar to those of the 2017 data. The power

production measured by the inverter was in good agreement with the 2017 weather data as well. However, it was observed that while there was a load running, the solar panel current would vary with the power drawn by the load, which is likely an artifact of how it is measured and accounts for the oscillations in inverter-measured PV power output. As mentioned previously, there were periods when the data from the inverter was not recorded, which account for the large gaps in portions of the figure.

5.3.3 Battery Energy Stored

The inverter did not directly output the battery energy levels. However, an estimation of the energy stored in the battery for the 7-day test was calculated using the battery voltage, charging, and discharging current reported by inverter. The relative change in energy between time increments was calculated according to Equation (*11*),

$$\Delta E_{stored}(t) = t_{int} \cdot v_{batt} \cdot (i_{chg} - i_{dsg}), \qquad (11)$$

where ΔE_{stored} is the change in stored energy over the time increment, t_{int} is the time interval between samples (1.94 seconds), v_{batt} is the battery voltage, i_{chg} is the battery charging current, and i_{dsg} is the battery discharge current. Whenever the battery voltage indicated that the batteries were fully charged ($v_{batt} \geq 144$ V), ΔE_{stored} was assumed zero. Because the data had gaps due to inverter data recording failures, the absolute positions of the battery energy curves were shifted such that their maxima were located at the full energy state of 16.2 kWh. These curves are plotted against the battery energy calculated from the simulated EDR energy power profile and simulated PV power profiles described in the previous sections according to Equations (*2*) and (*3*) (Figure 24).

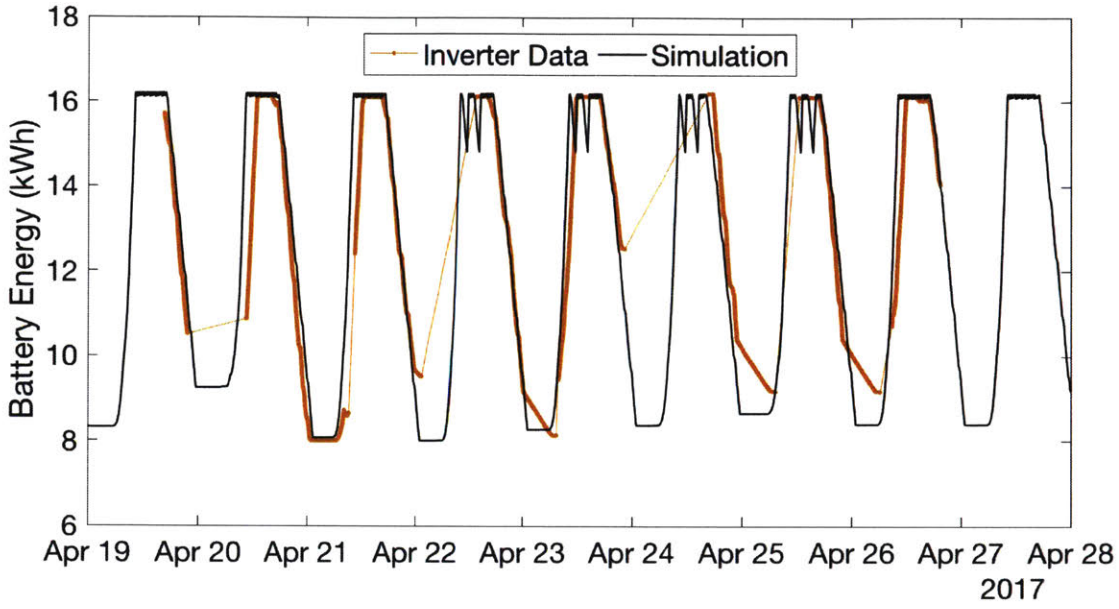

Figure 24. Battery Energy Stored

Comparison between the battery energy calculated from the data collected from the inverter in April 2017 (orange) and the expected battery energy based on the simulation model over the course of 2014 (black).

Due to inverter data collection failures, there was only one night over the course of the weeklong test during which the batteries appeared to be depleted to 50% discharge depth. However, the rates of charging and discharging of the batteries is a very close match to the model, which is a result of the agreement of the load power and PV panel power output from model to experiment.

CHAPTER 6

CONCLUSIONS AND FUTURE WORK

In this thesis, I investigated levers for reducing the cost of PV-powered systems with accumulable output, and applied my learnings in the design and analysis of a PV-powered electrodialysis desalination system which was installed in the field. I analyzed a theoretical reference system to understand general characteristics of PV-powered system design that could be applied to a wide range of applications, and focused on PV-EDR as a compelling design case. I found that system-level optimization considering the intermittent and diurnal characteristics of PV power allowed for lower-cost designs.

As a part of this work, I developed a PV-EDR model to take location-specific weather and water data and simulate the performance (water production quantity and quality) of a design consisting of off-the shelf components. I used a PSO to identify the lowest-cost PV-EDR system for Chelluru, a village near Hyderabad. This optimized design is expected to produce the requisite 10 m^3 of 300 mg/L salinity water per day, with a capital cost of $23,420. The optimized design, referred to as Design A, was compared to a PV-EDR system designed using a disaggregated approach and rules of thumb, referred to as Design B. Both designs, A and B, are expected to meet water demand requirements, but Design B has a much higher capital cost of $40,138. Because Design B was not designed to operate on PV power (the PV system was retrofitted to the EDR stack retroactively), Design B had an oversized, more expensive power system than what was achieved through the system optimization of Design A. Furthermore, the EDR stack of Design B was more expensive because of the greater number of membranes needed to complete water production in the 8-hour period selected based on current on-grid RO desalination systems.

I further used the PV-EDR model and optimization tools to investigate the parametric sensitivities of system capital cost to output reliability, feed and product water salinities, and individual component costs. I found that easing the output reliability constraint from 100% to 98% reduced the capital cost of the system by approximately 5.7%. This indicates that a handful of days during the least sunny time of the year drive up the system capital cost disproportionally. In realistic application of PV-EDR systems to supply village water needs, the desalination and power systems could be designed with lower output reliability if alternative water sources, such as trucked-in water, were available and economically feasible during those periods. Furthermore, it is expected that if water demand tracks with solar irradiance, as might be expected with water demand increasing during hotter months and decreasing during cooler, cloudier months, the energy and water buffering requirements would be reduced, which would further drive down the cost of the PV-EDR system. In this analysis, a constant water demand was assumed over the course of the year, because of a lack of seasonal water usage data for the region. The desalination system installed in Chelluru now has a sensor to track water withdrawal, and the data will be used in future work to more accurately simulate future PV-EDR designs, and likely contribute to cost reductions in the energy and water storage elements. Another design constraint imposed in this work was completely off-grid operation. In reality, many villages in India do have some grid connection, although it is unreliable enough that grid-reliant desalination is not a feasible option. A PV-EDR

system supplemented even minimally by grid electricity could help to ensure 100% output reliability with a lower capital cost.

To characterize the suitability of processes for PV power, I investigated operating flexibility and load sizing for a theoretical 8 kWh per day reference system and a PV-EDR system. I described the cost reductions afforded by operation flexibility of the load to better match the time-resolved solar irradiance, and the cost reductions enabled by designing power characteristics of the load to better suit an intermittent PV power source. The advantages of operation and load sizing flexibility are inherent in the optimization of PV-powered systems when the PV, batteries, and electrical load are optimized jointly subject to location-specific solar and weather data. This was a feature of the PV-EDR system design analyzed here, as well as previous work by Bilton, Smaoui, and others [21] [22]. However, to my knowledge the advantages of flexible operation and load sizing have not previously been compared to similar system designs with fixed operation schedules. I found that for my theoretical reference system operating 8 hours per day at 1 kW, flexible operation enabled a power system cost reduction of 39%. Designing the electrical load to operate for 6:45 hours per day enabled an additional power system cost reduction of 5%. If the electrical load had originally been designed to operate in excess of 12 hours per day, the cost reductions of electrical load sizing would have been much greater. This was the case for the PV-EDR system, which saw a power system cost reduction of 57.5% when the EDR system was resized and designed to operate for 8:35, rather than 17:42, hours per day. It should be noted that in these analyses, output reliability was set at 100% (an LPSP of 0) relative to a reference year. If the reliability constraint were eased, power system costs and storage requirements for both batteries and product can be further reduced.

The co-design of the electrical load and the power system illuminate the advantages of designing an electrical load that can perform the required task in a less-than-12-hour time period, enabling a smaller PV array and battery bank. When the load was not required to run at night on average, flexibility in the operating schedule reduced the amount of time the load needed to run in low-irradiance conditions. However, flexible operation requires product storage to meet a constant product demand over the annual cycle. The cost of product storage is very case-specific, and affects the relative favorability of flexible operation. If the cost of product storage over the year is less than the power system cost savings afforded by flexible operation (either intrinsically or due to a

positive correlation between product demand and solar irradiance), flexible operation will allow the overall system cost to be reduced.

Another important consideration is the scaling of electrical load with power rating. Higher-power loads that operate for fewer hours per day tend to cost more than smaller, low-power units that must run for longer to produce the same output. In the case of the PV-EDR system, the optimization favored a design with a smaller, lower-power, longer operation EDR unit because of the high current capital cost of the membranes. This acted as a counterbalance to the favorability of shorter operating times by the PV power system. However, if the cost of the electrical load is comparable to the power system as was the case for the EDR system with $20 membrane cell pairs, the overall system benefits from operating in a more favorable regime for intermittent and diurnal PV power. This observation is consistent with the high sensitivity of the PV-EDR system cost to the cost of the membranes.

Flexible operation and optimal load sizing approaches would be useful in reducing the cost of any PV-powered system with accumulable output and flexibility in operation schedule. For example, the PV power system of a drip irrigation system could be minimized with optimal sizing of the pumping unit, and flexible operation would allow the power profiles of the electrical load and PV power output to line up. This would reduce the cost of the power system substantially, and could reduce the cost of the system overall. Similarly, a municipal water supply with a water tower supplied by a PV-powered pump could be designed with these load sizing and operation flexibility principles to minimize its total cost. Incorporating PV power into these and other similar applications at reasonable cost would accelerate the adoption of PV into new areas. In the case of PV-EDR design, flexible operation and load sizing will become more useful tools for reducing power system cost as the capital cost of PV-EDR units decreases, and units operating less than 12 hours per day become comparable in cost to their associated power systems.

In this thesis, I have demonstrated that methods for modifying the power profile of the EDR system to more closely follow solar irradiance patterns can reduce the cost of the PV power system. Other methods for doing this include variable power pumping and variable voltage applied to the EDR stack, which are areas of future research in this project. If the magnitude of the power used to desalinate the water can more closely mimic the roughly parabolic solar power profile, the PV power system can be downsized in both the PV array and battery pack, and the power system

cost can be reduced. This is an important area of future research to aid system-level cost optimization of PV-powered systems.

The PV-EDR model described in this thesis predicted the performance of the Chelluru village desalination system during the 7-day testing period within 13%. This model will be useful for evaluating the performance and economic appeal of PV-EDR systems in other locations, and will continue to be improved through learnings from experimental testing and more sophisticated PV and battery device models. While the pilot PV-EDR system in Chelluru performed as predicted for the 7-day test, this period coincided with the sunniest time of the year. We would like to run the system for a year-long period to evaluate the accuracy of the model during different seasons. We would also like to evaluate other human-factors aspects of the design, such as the acceptability of the water to the village population and the ease of operation for the village operators. It will be important to understand the long-term performance of PV-EDR in the field, since it is not currently well understood.

I hope that the work described in this thesis will contribute to greater cost reductions in village-scale PV-EDR to make it a viable drinking water source in cost-constrained environments like India's rural villages. A greater goal of the system design framework presented here is its application to designing other PV-powered systems for affordability, persistency, reliability, and predictability. I expect that the flexible operation and load sizing design approaches detailed in this thesis will be useful for informing the design of any PV-powered system with accumulable output.

REFERENCES

[1] The World Bank, "Access to electricity, rural," [Online]. Available: http://data.worldbank.org/indicator/EG.ELC.ACCS.RU.ZS. [Accessed 9 May 2017].

[2] G. Gowrisankaran, S. S. Reynolds and M. Samano, "Intermittency and the Value of Renewable Energy," *Journal of Political Economy,* vol. 124, no. 4, pp. 1187-1234, August 2016.

[3] V. Bermudez, "Electricity storage supporting PV competitiveness in a reliable and sustainable electric network," *Journal of Renewable and Sustainable Energy,* vol. 9, 2017.

[4] A. I. Nikolaidis, Y. Koumparou, G. Makrides, V. Efthymiou, G. E. Georghiou and C. A. Charalambous, "Reliable integration of a concentrating solar power plant in a small isolated system through an appropriately sized battery energy storage system," *IET Renewable Power Generation,* vol. 10, no. 5, pp. 735-742, 2016.

[5] M. E. Glavin and W. G. Hurley, "Optimisation of a photovoltaic battery ultracapacitor hybrid energy storage system," *Solar Energy,* pp. 3009-3020, October 2012.

[6] A. Chaurey and T. C. Kandpal, "Assessment and evaluation of PV based decentralized rural electrification: An overview," *Renewable and Sustainable Energy Reviews,* vol. 4, no. 8, p. 2266–2278, 2010.

[7] E. Karakaya and P. Sriwannawit, "Barriers to the adoption of photovoltaic systems: The state of the art," *Renewable and Sustainable Energy Reviews,* vol. 49, p. 60–66, 2015.

[8] UNICEF and World Health Organization, "Progress on Sanitation and Drinking Water: 2015 Update and MDG Assessment," 2015.

[9] Central Ground Water Board, "Ground Water Quality in Shallow Aquifers of India," Government of India, 2010.

[10] Bureau of Indian Standards, "Drinking Water - Specification (Second Revision: IS 10500)," ISO 10500, 2012.

[11] Open Government Data Platform India, "Data.gov.in: Progress Report of Village Electrification as on May 2015," [Online]. Available: https://data.gov.in/visualize/?inst=e66ecc8f79fbde7c078b6c5f497efb80. [Accessed 28 February 2017].

[12] C. Chandramouli, "Census of India 2011 - Household Amenities and Assets: Source of Lighting," Government of India, 2012.

[13] N. Wright, "Justification of Village Scale Photovoltaic Powered Electrodialysis Desalination Systems for Rural India," Cambridge, 2014.

[14] N. C. B., 2016.

[15] N. C. Wright and A. G. Winter, V., "Justification for community-scale photovoltaic powered electrodialysis desalination systems for inland rural villages in India," *Desalination,* vol. 352, pp. 82-91, 2014.

[16] C. Olcan, "Multi-objective analytical model for optimal sizing of stand-alone photovoltaic water pumping systems," *Energy Conversion and Management,* vol. 100, pp. 358-369, May 2015.

[17] Y. Bakelli, A. H. Arab and B. Azoui, "Optimal sizing of photovoltaic pumping system with water tank storage using LPSP concept," *Solar Energy,* vol. 85, pp. 288-294, December 2011.

[18] A. H. A. Al Waeli, A. H. K. Al Kabi, A. Al Mamari, H. A. Kazem and M. T. Chaichan, "Evaluation of the Economic and Environmental Aspects of Using Photovoltaic Water Pumping System," in *9th International Conference on Robotic, Vision, Signal Processing and Power Applications*, 2016.

[19] R. Rawat, S. C. Kaushik and R. Lamba, "A review on modeling, design methodology and size optimization of photovoltaic based water pumping, standalone and grid connected system," *Renewable and Sustainable Energy Reviews,* vol. 57, p. 1506–1519, 2016.

[20] D. H. Muhsen, A. B. Ghazali and T. Khatib, "Multiobjective differential evolution algorithm-based sizing of a standalone photovoltaic water pumping system," *Energy Conversion and Management,* vol. 118, pp. 32-43, 2016.

[21] A. M. Bilton and L. C. Kelley, "Design of power systems for reverse osmosis desalination in remote communities," *Desalination and Water Treatment,* vol. 55, pp. 2868-2883, August 2015.

[22] M. Smaoui, A. Abdelkafi and L. Krichen, "Optimal sizing of stand-alone photovoltaic/wind/hydrogen hybrid system supplying a desalination unit," *Solar Energy,* vol. 120, pp. 263-276, 2015.

[23] K. Sundaramoorthy, "Development of the hard and soft constraints based optimisation model for unit sizing of the hybrid renewable energy system designed for microgrid applications," *International Journal of Sustainable Energy,* vol. 36, no. 2, 2014.

[24] A. H. Habib, V. Zamani and J. Kleissl, "Solar desalination system model for sizing of photovoltaic reverse osmosis (PVRO)," in *ASME 2015 Power Conference*, 2015.

[25] A. H. Habib, V. R. Disfani, J. Kleissl and R. A. de Callafon, "Optimal switchable load sizing and scheduling for standalone renewable energy systems," *Solar Energy,* vol. 144, pp. 707-720, 2017.

[26] L. B. Jaramillo and A. Weidlich, "Optimal microgrid scheduling with peak load reduction involving an electrolyzer and flexible loads," *Applied Energy,* vol. 169, pp. 857-865, 2016.

[27] T. Beck, H. Kondziella, G. Huard and T. Bruckner, "Assessing the influence of the temporal resolution of electrical load and PV generation profiles on self-consumption and sizing of PV-battery systems," *Applied Energy,* vol. 173, p. 331–342, 2016.

[28] M. R. Adiga, S. Adhikary, P. Narayanan, W. Harkare, S. Gomkale and K. Govindan, "Performance Analysis of Photovoltaic Electrodialysis Desalination Plant at Tanote in Thar Desert," *Desalination,* vol. 67, pp. 59-66, 1987.

[29] O. Kuroda, S. Takahashi, K. Wakamatsu, S. Itoh, S. Kubota, K. Kikuchi, Y. Eguchi, Y. Ikenaga, N. Sohma and K. Nishinoiri, "An Electrodialysis Sea Water Desalination System Powered By Photovoltaic Cells," *Desalination,* vol. 65, pp. 161-169, 1987.

[30] N. Soma, F. Kanenobu, S. Inoue and O. Kuroda, "The practical operation of photovoltaic desalination systems," *International Journal of Solar Energy,* vol. 13, pp. 97-109, 1992.

[31] A. Bilton, "A Modular Design Architecture for Application to Community-Scale Photovoltaic-Powered Reverse Osmosis Systems," Cambridge, 2006.

[32] A. M. Bilton and L. C. Kelley, "Design of power systems for reverse osmosis desalination in remote communities," *Desalination and Water Treatment,* vol. 55, no. 10, pp. 2868-2883, 2015.

[33] P. Denholm and R. M. Margolis, "Evaluating the limits of solar photovoltaics (PV) in electric power systems utilizing energy storage and other enabling technologies," *Energy Policy,* pp. 4424-4433, 2007.

[34] National Renewable Energy Laboratory (NREL), "NSRDB Data Viewer," [Online]. Available: https://maps.nrel.gov/nsrdb-viewer/. [Accessed 16 September 2016].

[35] "Suniva Optimus Series Monocrystalline Solar Modules," [Online]. Available: https://www.wholesalesolar.com/cms/suniva-suniva-opt330-72-4-100-silver-mono-solar-panel-specs-1610309543.pdf. [Accessed 20 May 2016].

[36] N. Pearsall, Ed., The Performance of Photovoltaic (PV) Systems: Modelling, Measurement and Assessment, vol. 105, Woodhead Publishing, 2017.

[37] B. S. Borowy and Z. M. Salameh, "Methodology for Optimally Sizing the Combination of a Battery Bank and PV Array in a Wind/PV Hybrid System," *IEEE Transactions on Energy Conversion,* vol. 11, no. 2, pp. 367-375, 1996.

[38] T. Linden and T. B. Reddy, Handbook of Batteries, 3rd Edition ed., New York: McGraw-Hill, 2002.

[39] N. S. Shrikhande, Bengaluru, 2016.

[40] R. N. Chapman, Sizing Handbook for Stand-Alone Photovoltaic/Storage Systems, Albuquerque, NM: Sandia National Laboratories, 1987.

[41] N. C. Wright, G. D. Van de Zande and A. Winter, "Design of a Village-Scale PV Powered Electrodialysis Reversal System for Brackish Water Desalination in India," in *The International Desalination Association World Congress on Desalination and Water Reuse*, San Diego, 2015.

[42] N. C. Wright, S. R. Shah and A. G. Winter, V, "Validated Model of the Desalination and Pumping Energetic Requirements of Brackish Water Electrodialysis at Multiple Size Scales (in preparation)".

[43] J. M. Ortiz, J. A. Sotoca, E. Exposito, F. Gallud, V. Garca-Garca, V. Montiel and A. Aldaz, "Brackish water desalination by electrodialysis: Batch recirculation operation modeling," *Journal of Membrane Science,* vol. 252, pp. 65-75, 2005.

[44] H. Strathmann, "Electrodialysis, a mature technology with a multitude of new applications," *Desalination,* vol. 264, no. 3, pp. 268-288, 2010.

[45] Y. Tanaka, Ion Exchange Membrane Electrodialysis: Fundamentals, Desalination, Separation, Nova Science Publishers, 2010.

[46] General Electric Water & Process Technologies, "GE Water & Process Technologies Document Library," 1998. [Online]. Available: https://www.gewater.com/kcpguest/document-library.do.

[47] A. Rose, A. Campanella, R. Amatya and R. stoner, "Solar Power Applications in the Developing World," *The MIT Future of Solar Energy Study Working Paper,* January 2015.

[48] General Electric Water & Process Technologies, Westborough, MA, 2014.

[49] N. CB, 2016.

[50] J. Kennedy and R. Eberhart, "Particle Swarm Optimization," in *Proceedings of the IEEE International Conference on Neural Networks*, Perth, 1995.

[51] "Off-Grid System Sizing," [Online]. Available: http://www.affordable-solar.com/learning-center/solar-basics/off-grid-system-sizing/. [Accessed 12 May 2017].

[52] National Renewable Energy Laboratory, "India Solar Resource - Global Horizontal Irradiance," [Online]. Available: http://www.nrel.gov/international/images/india_ghi_annual.jpg . [Accessed 14 March 2017].

[53] "How to Design Solar PV System," [Online]. Available: http://www.leonics.com/support/article2_12j/articles2_12j_en.php. [Accessed 15 March 2017].

[54] Hangzhou Iontech Environmental Technology Company Limited, Hangzhou, 2014.

[55] J. Ortiz, E. Expósito, F. Gallud, V. Garcia-Garcia, V. Montiel and A. Aldaz, "Photovoltaic electrodialysis system for brackish water desalination: Modeling of global process," *Journal of Membrane Science,* vol. 274, pp. 138-149, 2006.

[56] J. M. Ortiz, J. A. Sotoca, E. Exposito, F. Gallud, V. Garca-Garca, V. Montiel and A. Aldaz, "Brackish water desalination by electrodialysis: Batch recirculation operation modeling," *Membrane Science,* vol. 252, pp. 65-75, 2005.

[57] Hangzhou Iontech Environmental Technology Company Limited, Hangzhou, 2014.